Supporting Information

Potential Pharmacological Chaperones Targeting Cancer-Associated MCL-1 and Parkinson's Disease-Associated α-Synuclein

Misook Oh,[*,†,1] Ji Hoon Lee,[†,1] Wei Wang,[*,‡] Hui Sun Lee,[§] Woo Sirl Lee,[†] Christopher Burlak,[¶] Wonpil Im,[§] Quyen Hoang,[*,‡,2] and Hyun-Suk Lim[*,†,2]

[*]Department of Biochemistry and Molecular Biology, Indiana University School of Medicine, Indianapolis, Indiana, United States of America, [†]Department of Chemistry, Pohang University of Science and Technology (POSTECH), Pohang 790-784, South Korea, [‡]Stark Neurosciences Research Institute, Indiana University School of Medicine, Indianapolis, Indiana, United States of America, [§]Department of Molecular Biosciences and Centre for Bioinformatics, The University of Kansas, Lawrence, Kansas, United States of America, [¶] Department of Surgery, Indiana University School of Medicine, Indianapolis, Indiana, United States of America

[1]M.O. and J.H.L. contributed equally to this work

[2]To whom correspondence may be addressed:

Table of contents

Materials and General Methods:

Chemical reagents purchased from commercial suppliers were used without further purification. TentaGel B NH_2 / Boc resin (130 µm, 0.25 mmol/g) and TentaGel S NH_2 resin (130 µm, 0.29 mmol/g) were purchased from Rapp Polymere. Rink amide MBHA resin (0.96 mmol/g) was purchased from Novabiochem. LC/MS characterization was performed on an Agilent 1200 LC/MS system (Agilent Technology) with a C18 reversed phase column (Kinetex, 2 µm, 4.6 mm × 50 mm). A gradient elution of 90% A in 2 min followed by 100% B in 14 min was used at flow rate of 0.8 mL/min (solvent A: 95% H_2O, 5% MeOH, 0.01% TFA; B: MeOH, 0.01% TFA). Preparative HPLC purification was performed on an Agilent 1120 Compact LC system (Agilent Technology) with a C18 reversed phase column (Agilent Technology, 5 µM, 25 mm x 125 mm) using a linear gradient from 10% B to 100% B by changing solvent composition over 40 minutes. MALDI-TOF MS was performed on ABI 4800 and ABI 5800 mass spectrometers (Applied Biosystems) using α-cyano-4-hydroxycinnamic acid as a matrix.

General procedure for solid-phase synthesis:

Rink amide MBHA resin (100 mg, 69 µmol) was swelled with DMF (2 mL) in a 5 mL fritted syringe for 1 h. The Fmoc protecting group was deprotected by treating with 20 % piperidine in DMF (2 × 10 min). After thorough washing with DMF (3×), MeOH (2×), CH_2Cl_2 (2×), and DMF (3×), mono-substituted dichlorotriazines **3** was loaded on the resin by reacting with Et_3N (5 equiv) in DMF (1 mL) at room temperature overnight. Next, nosyl-protected piperazine derivatives **5** (10 equiv) were coupled to the resin-bound triazine derivatives **4** by in the presence of Et_3N (5 equiv) in DMF at 60℃ overnight. Note that beads were drained and thoroughly washed with DMF (3×), MeOH (2×), CH_2Cl_2 (2×), and DMF (3×) at the end

of each reaction step unless otherwise noted. The *N*-Ns protecting group on **6** was removed by treating with 2-mercaptoethanol (20 equiv) and DBU (10 equiv) in DMF at room temperature for 2 hr. Subsequently, 2-ethylamino-4,6-dichloro-[1,3,5]triazine **7** was introduced to afford **8** by treating the beads with **7** (5 equiv) and DIEA (5 equiv) in NMP at 60℃ overnight. The chloride was then displaced with various amines (R_3R_3'NH). Finally, cleavage reaction with trifluoroacetic acid (TFA) furnished tri-functionalized triazine-piperazine-triazine compounds **9**. The identity and purity of the small molecules were confirmed by LC/MS analysis.

General procedure for library synthesis:

TentaGel B NH_2 / Boc resins (250 mg, NH_2: 62.5 μmol / Boc: 1.3 μmol) were swollen in DMF (2 mL) for 2 h. The beads were treated with Fmoc-L-methionine (Fmoc-Met-OH) (5 equiv) in the presence of HOBt (5 equiv), HBTU (5 equiv) and DIEA (10 equiv) in DMF (1 mL) at room temperature. After shaking for 2 h, the reaction mixture was drained and washed with DMF (3×), MeOH (2×), CH_2Cl_2 (2×), and DMF (3×). The Fmoc protecting group was removed by treating the resins with 20 % piperidine in DMF (1 mL, 2 × 10 min). Next, Fmoc-4-aminobutyric acid (Abu) (5 equiv) was added using the same peptide coupling conditions. This process was repeated two times to couple three Abu linker residues. After Fmoc deprotection, the resulting amines were bromoacetylated by treating with 1 M bromoacetic acid and 1 M DIC in DMF (2 mL) at room temperature. The beads were then divided into 18 reaction vessels in equal amounts, and each portion was treated with 18 different amines (2M amine in 2 mL DMF) at room temperature for 2 hr. The N-termini of the peptoids were protected with allyloxycarbonyl (Alloc) group by treating with allyl chloroformate (5 equiv) and Et_3N (6 equiv) in anhydrous CH_2Cl_2 at 4℃ overnight. Next, the

Boc group in the exterior of the beads was eliminated by treating with 50 % TFA in CH_2Cl_2 for 1 h. The resulting primary amines were coupled with 18 different mono-substituted triazine derivatives **4** (5 equiv). After thorough washing with DMF (3×), MeOH (2×), CH_2Cl_2 (2×) and NMP (3×), all the beads were pooled in a 250 mL vessel for randomization and then split into 3 vessels. The chloride on the triazine **12** was displaced with three different piperazines **13** by reacting with Boc protected piperazines (10 equiv) in DIEA (10 equiv) and NMP (1 mL) at 60°C overnight. After washing with DMF (3×), MeOH (2×), CH_2Cl_2 (2×), the Alloc group was removed by treatment with $Pd(PPh_3)_4$ (0.2 equiv) and $PhSiH_3$ (10 equiv) in anhydrous CH_2Cl_2 (1 mL). Using the submonomer route, second peptoid residues (R_2") were coupled. The beads were again pooled for randomization. After bromoacetylation, the beads were split into 27 vessels and reacted with 27 different amines. N-termini of the peptoids were blocked by bromoacetylation and subsequent reaction with piperidine. Next, the Boc group on **14** was removed by treatment with 50 % TFA in CH_2Cl_2 for 1 h. After neutralization with 10% DIEA in DMF, to the beads were added 4,6-dichloro-1,3,5-triazin-2-ethylamine with DIEA in NMP at 60°C for overnight. After washing with DMF (3×), MeOH (2×), CH_2Cl_2 (2×) and NMP (3×), the beads were treated with 27 different amines (R_3R_3'NH) DIEA and NMP at 60°C overnight. After washing with DMF (3×), MeOH (2×), CH_2Cl_2 (2×), all the beads were mixed together and treated with 95% TFA for global deprotection. For cleavage, the individual beads were treated with 20 μL of CNBr (40 mg/mL) in ACN/AcOH/H_2O (5:4:1) at room temperature for 12h. To examine the efficiency of the library synthesis, 30 beads were randomly picked from the library. After cleavage reaction with CNBr, the resulting peptoids were analyzed by MS. Note that α-helix mimetic molecules on the suface are not cleavable and only peptoids attached to the beads through Methionine are released upon CNBr treatment. All the tested beads showed high purity products without

significant impurity peaks, reflecting the efficiency of the library synthesis.

Synthesis of fluorescently-labeled compounds (9a-c-FL, Q1-2-FL):

TentaGel S NH_2 resin (100 mg, 29 μmol) was swollen in DMF (2 mL) for 1 hr. The beads were treated with Fmoc-Met-OH (5 equiv) in the presence of HOBt (5 equiv), HBTU (5 equiv) and DIEA (10 equiv) in DMF (1 mL) at room temperature. After shaking for 2 hr, the reaction mixture was drained and washed. The Fmoc protecting group was removed by treating with 20 % piperidine in DMF (1 mL, 2 × 10 min). Subsequently, Fmoc-Lys(Alloc)-OH and Fmoc-Abu-OH were coupled under the same peptide coupling conditions. After deprotection of Fmoc group, the resins were treated with mono-substituted dichlorotriazines **3** (5 equiv) and DIEA (5 equiv) in DMF at room temperature overnight. The reaction mixture was drained and washed with DMF (3×), MeOH (2×), CH_2Cl_2 (2×) and NMP (3×). To the beads in NMP (1 mL) were added Boc protected piperazine derivatives (10 equiv) and DIEA (10 equiv). The mixture was stirred at 60°C overnight. After washing, the Boc group was removed by treatment with 50 % TFA in CH_2Cl_2 for 1 hr. The resins were neutralized with 10% DIEA in DMF (1 mL) for 1hr and washed with DMF (3×), MeOH (2×), CH_2Cl_2 (2×) and NMP (3×). Next, the beads were treated with 4,6-dichloro-1,3,5-triazin-2-ethylamine (5 equiv) and DIEA (5equiv) in NMP at 60°C overnight and then washed with DMF (3×), MeOH (2×), CH_2Cl_2 (2×) and NMP (3×). The resins were then treated with an amine (20 equiv) and DIEA (20 equiv) in NMP at 60°C overnight and washed with DMF (3×), MeOH (2×), CH_2Cl_2 (2×). After Alloc deprotection by treating with $Pd(PPh_3)_4$ (0.2 equiv) and $PhSiH_3$ (10 equiv) in anhydrous CH_2Cl_2 (1 mL) for 1 hr, the resulting NH_2 on Lys residue was couepled with 5,6-carboxyfluorescein (5 equiv) using peptide coupling conditions. For cleavage, the beads were treated with 1 mL of CNBr (40 mg/mL) in ACN/AcOH/H_2O (5:4:1) at room temperature for

12 hr. The cleaved crude products were purified by HPLC.

Synthesis of 9 and Q compounds. Rink amide MBHA resin (100 mg, 93 μmol) was swelled with DMF (2 mL) in a 5 mL fritted syringe for 1 hr. The Fmoc protecting group was deprotected by treating with 20 % piperidine in DMF (2 × 10 min). After thorough washing with DMF (3×), MeOH (2×), CH_2Cl_2 (2×), and DMF (3×), mono-substituted dichlorotriazines was loaded by reacting with **3** (5 equiv) and DIEA (5 equiv) in DMF (1 mL) at room temperature overnight. Next, nosyl-protected piperazine derivatives **5** were coupled to the resin-bound triazine derivatives **4** by reacting with **5** (10 equiv) and Et_3N (5 equiv) in DMF at 60℃ overnight. Beads were drained and thoroughly washed with DMF (3×), MeOH (2×), CH_2Cl_2 (2×), and DMF (3×) at the end of each reaction step unless otherwise noted. The *N*-Ns protecting group on **6** was removed by treating with 2-mercaptoethanol (20 equiv) and DBU (10 equiv) in DMF at room temperature for 2 hr. Subsequently, 2-ethylamino-4,6-dichloro-[1,3,5]triazine **7** was introduced to afford **8** by treating the beads with **7** (5 equiv) and DIEA (5 equiv) in NMP at 60℃ overnight. The chloride was then displaced with various amines (R_3R_3'NH). Finally, cleavage reaction with trifluoroacetic acid (TFA) furnished triazine-piperazine-triazine compounds **9**. Q1 and Q2 compounds were synthesized using the same procedure described above. The identity and purity of the crude compounds were confirmed by LC/MS analysis. The compounds were purified by reverse-phase HPLC, and further characterized by ^{1}H-NMR, ^{13}C-NMR, and HRMS.

6-(4-(4-amino-6-((benzo[*d*][1,3]dioxol-5-ylmethyl)amino)-1,3,5-triazin-2-yl)-2-benzylpiperazin-1-yl)-N^2-benzyl-N^4-ethyl-1,3,5-triazine-2,4-diamine·TFA (9a). Yield: 25.8 mg (43 %) from 100 mg of resin. ^{1}H-NMR (500 MHz, methanol-d_4) δ 1.26 (m, 3H) 2.61-2.77 (m, 2H), 3.05-3.15 (m, 2H), 3.31-3.35 (m, 3H), 4.31 (m, 1H), 4.45-4.65 (m, 6H),

5.04 (m, 1H), 5.71 (d, *J* = 36.0 Hz, 1H), 5.83 (d, *J* = 3.5 Hz, 1H), 6.65-6.81 (m, 3H), 6.98-7.08 (m, 5H), 7.19 (m, 1H), 7.25-7.27 (m, 4H); ^{13}C-NMR (126 MHz, $CDCl_3$) δ 14.4, 35.9, 39.1, 43.4, 44.3, 44.5, 44.7, 53.2, 53.5, 55.3, 101.2, 107.9, 108.4, 120.8, 121.1, 127.0, 127.5, 127.7, 128.5, 128.8, 129.2, 130.7, 136.9, 137.2, 147.2, 147.9, 155.7, 156.2, 157.5, 162.6; HRMS (ESI) calculated for $C_{34}H_{39}N_{12}O_2$ $[M + H]^+$: 647.3319; Found: 647.3319.

6-(4-(4-amino-6-((cyclopropylmethyl)(propyl)amino)-1,3,5-triazin-2-yl)-2-benzylpiperazin-1-yl)-N^2-(benzo[*d*][1,3]dioxol-5-ylmethyl)-N^4-ethyl-1,3,5-triazine-2,4-diamine·TFA (9b). Yield: 18.8 mg (31 %) from 100 mg of resin. ^{1}H-NMR (500 MHz, methanol-d_4) δ 0.40 (m, 2H), 0.62 (m, 2H), 1.00 (m, 3H), 1.12 (br s, 1H), 1.25 (t, *J* = 7.5 Hz, 3H), 1.72 (m, 2H), 2.91-3.00 (m, 2H), 3.33 (m, 2H), 3.49-3.56 (m, 7H), 4.46-4.61 (m, 4H), 4.73 (m, 1H), 5.19 (m, 1H), 5.91 (s, 1H), 5.94 (s, 1H). 6.76-6.88 (m, 3H), 7.13 (d, *J* = 6.5 Hz, 1H), 7.20-7.25 (m, 4H); ^{13}C-NMR (126 MHz, $CDCl_3$) δ 3.7, 9.3, 9.6, 10.7, 11.5, 14.4, 20.9, 35.9, 39.1, 43.4, 44.3, 49.4, 50.1, 51.8, 52.9, 55.4, 101.2, 107.6, 108.3, 120.4, 121.1, 127.1, 128.6, 129.2, 130.0, 130.8, 131.0, 136.9, 147.2, 148.1, 155.6, 156.0, 158.2, 162.6; HRMS (ESI) calculated for $C_{34}H_{45}N_{12}O_2$ $[M + H]^+$: 653.3788; Found: 653.3787.

4-(2-((4-(4-(4-amino-6-((4-phenoxyphenyl)amino)-1,3,5-triazin-2-yl)-2-benzylpiperazin-1-yl)-6-(ethylamino)-1,3,5-triazin-2-yl)amino)ethyl)phenol·TFA (9c). Yield: 27.0 mg (41 %) from 100 mg of resin. ^{1}H-NMR (500 MHz, methanol-d_4) δ 1.25 (m, 3H), 2.82 (m, 2H), 2.91(br s, 2H), 3.30 (m, 2H), 3.49 (m, 3H), 3.66 (m, 2H), 4.57-4.68 (m, 3H), 5.13 (m, 1H), 6.73 (m, 2H), 6.90 (br s, 1H), 7.03-7.07 (m, 6H), 7.17-7.24 (m, 5H) 7.41 (m, 3H), 7.58 (br s, 1H); ^{13}C-NMR (126 MHz, DMSO-d_6) δ 14.6, 14.8, 34.2, 35.7, 36.0, 42.5, 43.2, 44.1, 53.9, 115.6, 118.7, 119.5, 122.9, 123.7, 126.7, 128.7, 129.2, 129.6, 130.0, 130.1, 130.5, 138.2,

152.5, 155.1, 155.4, 156.3, 157.6, 162.1, 163.8; HRMS (ESI) calculated for $C_{39}H_{43}N_{12}O_2$ [M + H]$^+$: 711.3632; Found: 711.3613.

6-(4-(4-amino-6-(ethylamino)-1,3,5-triazin-2-yl)piperazin-1-yl)-N^2,N^4-diethyl-1,3,5-triazine-2,4-diamine·TFA (9-nc). Yield: 18.0 mg (50 %) from 100 mg of resin. ^{1}H-NMR (500 MHz, methanol-d_4) δ 1.14 (t, J = 7.0 Hz, 9H), 3.38 (m, 6H), 3.89 (br s, 8H); ^{13}C-NMR (126 MHz, DMSO-d_6) δ 14.6, 35.7, 43.4, 155.8, 157.4, 162.1; HRMS (ESI) calculated for $C_{16}H_{29}N_{12}$ [M + H]$^+$: 389.2638; Found: 389.2631.

6-(4-(4-amino-6-(4-phenoxyphenylamino)-1,3,5-triazin-2-yl)-2-benzylpiperazin-1-yl)-*N*^{2}-(benzo[*d*][1,3]dioxol-5-ylmethyl)-*N*^{4}-ethyl-1,3,5-triazine-2,4-diamine·TFA (Q1). ^{1}H-NMR (600 MHz, $CDCl_3$) δ 1.28 (m, 3H) 2.80-2.86 (m, 2H), 3.14-3.22 (m, 2H), 3.36-3.43 (m, 1H), 3.48-3.53 (m, 2H), 4.50-4.56 (m, 2H), 4.63-4.77 (m, 3H), 5.12 (bs, 1H), 5.93-5.98 (m, 2H), 6.76-6.89 (m, 4H), 7.01-7.20 (m, 7H), 7.26-7.29 (m, 1H), 7.38-7.41 (m, 3H), 7.58 (dd, J = 3.0, 9.0 Hz, 1H), 7.76-7.82 (m, 1H), 8.05-8.16 (m, 1H), 10.58 (m, 1H), 14.59 (bs, 1H); ^{13}C-NMR (150 MHz, $CDCl_3$) δ 14.3, 35.9, 36.2, 39.1, 39.2, 43.6, 44.2, 44.5, 53.4, 101.2, 107.6, 108.4, 118.9, 120.4, 121.0, 123.2, 123.7, 127.1, 128.6, 129.0, 129.3, 129.8, 131.3, 136.7, 147.2, 148.1, 154.2, 154.7, 155.8, 156.2, 157.0, 157.6, 162.5; HRMS (ESI) calculated for $C_{39}H_{41}N_{12}O_3$ [M + H]$^+$: 725.3425; Found: 725.3427.

6-(4-(4-amino-6-(4-phenoxyphenylamino)-1,3,5-triazin-2-yl)-2-benzylpiperazin-1-yl)-*N*^{2}-(3,4-dimethoxybenzyl)-*N*^{4}-ethyl-1,3,5-triazine-2,4-diamine·TFA (Q2). ^{1}H-NMR (600 MHz, $CDCl_3$) δ 1.28 (m, 3H) 2.81-2.86 (m, 2H), 3.16-3.22 (m, 2H), 3.36-3.43 (m, 1H), 3.47-3.51 (m, 2H), 3.80-3.91 (m, 5H), 4.55-4.59 (m, 2H), 4.65-4.69 (m, 2H), 4.74-4.76 (m, 1H),

5.12 (bs, 1H), 6.81-6.89 (m, 4H), 7.00-7.21 (m, 7H), 7.26-7.29 (m, 1H), 7.38-7.41 (m, 3H), 7.58 (dd, *J* = 3.0, 9.0 Hz, 1H), 7.69-7.77 (m, 1H), 8.23-8.30 (m, 1H), 10.58 (m, 1H), 14.31 (bs, 1H); ^{13}C-NMR (150 MHz, $CDCl_3$) δ 14.3, 35.9, 36.3, 39.2, 43.6, 44.3, 44.5, 53.4, 55.9, 110.6, 110.1, 111.3, 118.9, 119.1, 119.4, 119.9, 123.2, 123.6, 127.1, 128.6, 129.0, 129.3, 129.9, 131.3, 136.7, 148.7, 149.3, 154.2, 154.7, 155.7, 156.0, 157.0, 157.5, 162.5; HRMS (ESI) calculated for $C_{40}H_{40}N_{12}O_3$ $[M + H]^+$: 741.3748; Found: 741.3741.

Computational Molecular Docking. Computational molecular docking experiments were carried out to investigate the binding modes of **9c** on MCL-1ΔNΔC (Fig. S5). The initial structures of **9c** were built using Maestro (Maestro v9.0, Schrödinger, LLC, Portland, OR) and subjected to energy-minimization with the CHARMM General Force Field (Vanommeslaeghe, K; Hatcher, E.; Acharya, C.; Kundu, S.; Zhong, S.; Shim, J.; Darian, E.; Guvench, O.; Lopes, P.; Vorobyov, I.; Mackerell, A. D. *J. Comput. Chem.* **2010**, *31*, 671). Preprocessing of ligand and receptor structures for docking was implemented using Raccoon (Forli, S. Raccoon|Autodock VS: an automated tool for preparing AutoDock virtual screenings). The coordinates of the docking box center were determined by the geometric center of the BH3 helix residues 9−16 and the box sizes were set to 25 Å in *X*, *Y*, and *Z*. To generate a set of pose decoys in the MCL-1ΔNΔC crystal structure (PDB entry: 3MK8), we performed independent 20 AutoDock Vina (Trott, O.; Olson, A. J. *J. Comput. Chem.* **2010**, *31*, 455) docking runs with different initial random numbers for each compound. 400 pose decoys for each compound were obtained from the docking experiments and the final model was determined from the best scoring pose. Software PyMol was used for the molecular visualization. In Fig. S7, MCL-1ΔNΔC is shown in an electrostatic surface representation with red for negatively-charged residues and blue for positively-charged residues.

MCL-1 Protein Purification/Biotinylation. The expression plasmids encoding BH3-binding domain of human MCL-1ΔNΔC (a.a. 172-320) tagged with GST (provided by Dr. Loren Walensky) were transformed into BL21 (DE3) *E. coli* cells. MCL-1 protein purification was carried out as previously described (70). MCL-1 protein was then biotinylated by incubating with sulfo-NHS-Biotin (Thermo Scientific) in 0.1 M $NaHCO_3$ buffer (pH 8.3) for 45 min at room temperature (Note that MCL-1ΔNΔC used for the experiment has several lysine residues which are facing the outside and away from the BH3 binding active site. Thus, we used MCL-1ΔNΔC without modification for biotinylation). The reaction was stopped by adding 1.5 M hydroxylamine. The labeled protein was separated by dialyzing against 1xPBS buffer containing 0.05% Tween20 (pH 7.4). Degree of labeling was determined according to the manufacturer's instruction (degree of biotinylation: 1.05 biotin per protein).

General procedure for on-bead screening: For selection of the best ligands for a target protein from the library molecules, we executed two rounds of on-bead screens using magnetic separation followed by alkaline phosphatase (AP)-based detection. First, 25 mg (≈ 10,200 beads, ≈ 7 copies of diversity) of the library beads were screened for their binding ability to the target protein by incubating the library beads with 200 nM of a biotinylated protein overnight at 4°C. After washing unbound protein followed by exposure to streptavidin (SA)-coupled Dynabeads (iron oxide particles), the positive beads were selected by magnetic separation. From this first round of screening, several hundred beads were selected. We note that SA-binding beads (potential false positives) were eliminated prior to the screen with the target protein by incubating the beads with SA-coupled Dynabeads. The selected beads were stripped of bound proteins by boiling in 1% SDS. After washing, the beads were again

incubated with 100 nM of the biotinylated target protein for 4 hours at 4°C followed by probing with SA-conjugated AP. It is of note that more stringent conditions (fewer amounts of protein and shorter incubation time) were employed in the second round of screening to select best compounds. The beads were then treated with 5-bromo-4-chloro-3-indolyl phosphate, a substrate for colorimetric detection of alkaline phosphatase. The most blue-colored beads were isolated as putative hits. Peptoids released from individual beads were sequenced by MS/MS. Chemical structures of the corresponding triazine-piperazine-triazines were unambiguously decoded by the coding peptoid sequences. For further studies, the hit compounds were re-synthesized and purified by HPLC.

α-Synuclein Protein Purification/Biotinylation. The construnct of a-synuclein with an N-terminal extension MKCK quad-peptide open reading frame was amplifyed from a pRS vector containing full-length wild-type by PCR using a forward primer containing a SamI restriction site (5′- GGAATTCCCGGGAATG-TGTGTATTCTGCAAAGGACTTTCAAAGGC-3′) and a reverse primer containing an Xho1 restriction site (5′- GCCTTTGAAAGTCCTTTGCAGAATACACACATTCCCGGGAATT-CC-3′). The amplified DNA was cloned into a pGEX-6P-1 plasmid (GE Biosciences), thus creating a GST fusion construct. The expression plasmids were transformed into rossetta 2 (DE3) *E. coli* cells, and protein expression was induced with 1 mM isopropyl β-D-1-thiogalactopyranoside (IPTG) at 20 ºC . Cell pellets were resuspended in lysis buffer (100 mM HEPES, pH =7.4, 150 mM NaCl, 10% glycerol, 0.1% BOG, Halt Protease Inhibitor cocktail (Thermo Scientific)) and lysed by sonication. After centrifugation, cell lysates were applied to a 20-mL GSTPrep column (GE Life Sciences) according to the manufacturer's instructions. A-synuclein protein was obtained by cleavage reaction by PreScission protease

(GE healthcare life sciences) overnight. After buffer exchange, another round of loading to GSTprep column to remove GST, and passing through the size exclusion chromatography. a-Synuclein protein was then biotinylated by incubating with sulfo-NHS-Biotin (Thermo Scientific) in 0.1 M $NaHCO_3$ buffer (pH 8.3) for 45 min at room temperature. The reaction was stopped by adding 1.5 M hydroxylamine. The labeled protein was separated by dialyzing against 1xPBS buffer containing 0.05% Tween20 (pH 7.4). Degree of labeling was determined according to the manufacturer's instruction (degree of biotinylation: 1.07 biotin per protein).

Fluorescence Polarization Assays. The fluoresceinated compounds **9a-c-FL** (50 nM) were incubated with indicated concentrations of MCL-1ΔNΔC or BCL-XLΔC protein in binding buffer (50 mM Tris, 100 mM NaCl, pH 8.0) at room temperature for 30 min in the dark. The fluorescence polarization values were measured on a SpectraMax® M5 Multi-Mode Microplate Reader (Molecular Devices). Excitation wavelength was 485 nm, and emission was detected at 535 nm. The K_D was calculated using GraphPad Prism® 4 software. For competitive FP experiments, we monitored the displacement of FITC-labeled MCL-1 BH3 peptide (FITC-MCL-1-BH3 peptide) from MCL-1ΔNΔC by **9a-c** or **9-nc**. The N-terminally labeled FITC-MCL-1-BH3 peptide (FITC-Abu-KALETLRRVGDGVQRNHETAF-NH2) was synthesized by standard Fmoc chemistry and purified by HPLC. FITC-MCL-1-BH3 (50 nM) was incubated with 0.8 μM of MCL-1ΔNΔC in binding buffer for 30 min, and then varying concentrations of **9a-c** or **9-nc** were added. After incubation for another 30 min, the fluorescence polarization values were measured. K_i values were calculated as described previously (Nikolovska-Coleska, Z. et al, *Anal. Biochem*. **2004**, *332*, 261).

Cell viability assays. Jurkat T cells were maintained in RPMI 1640 medium (ATCC) supplemented with 10% FBS and 4 x10^4 cells were seeded in 96-well plates in 100 μL of Opti-MEM medium (Invitrogen) for cell viability assay. WS-1 cells were maintained in MEM medium supplemented with 10% FBS and 2 x 10^4 cells were plated in 96-well plates in 100 μL of MEM medium with 10% FBS for 24 hr, washed with PBS, and then incubated in 100 μL of Opti-MEM medium for cell viability assay. Cells were serum-starved for 6 hr and treated with **9c**. After incubation for 24 hr, cell viability was measured by CellTiter 96 AQueous Non-Radioactive Cell Proliferation Assay kit (Promega) according to the manufacturer's instruction.

Caspase Assays. Jurkat T cells were plated at 2 x10^4 cells/well in white-walled 96-well plates in Opti-MEM medium and treated with varying concentrations of **9c** and **9-nc** or DMSO for 16 hrs. WS-1 cells were plated at 1x10^4 cells/well in white-walled 96-well plates and cultured for 24 hs in MEM with 10% FBS. Cells were washed with PBS and then treated with compounds in Opti-MEM medium as Jurkat T cells. The caspase 3/7 activity was measured using Caspase-Glo 3/7 Assay kit (Promega) according to the manufacturer's instructions.

Confocal microscopy experiment: A549 cells **(**5 x 10^3 cells) were plated in 96-well plates in 100 μl of MEM medium with 10% FBS for A549 cells. Cells were maintained for 24 hr, washed with PBS, and then were incubated with 1 μM of **9c-FL**, or 5(6)-carboxyfluorescein in Opti-MEM medium for 2.5 hr. The fluorescence images were taken after the cells were washed with 1× PBS (2 times).

Co-immunoprecipitation assay. Jurkat T cells (1×10^7 cells) were treated with DMSO or increasing concentrations of **9c** in Opti-MEM medium. After incubation for 2.5 hr, cells were harvested, washed with PBS twice, and lysed on ice with lysis buffer (50 mM Tris-HCl, pH 7.4, 150 mM NaCl, 1 mM EDTA, 1 mM DTT, 0.5% NP-40, and complete protease inhibitor tablet). Pre-cleared cell lysates were incubated with anti-MCL-1 antibody (S-19, Santa Cruz) at 4°C overnight, followed by protein A/G agarose incubation for 1 hr. The beads were precipitated and washed with lysis buffer three times, and the denatured proteins were then subjected to Western blot using anti-BAK (Cell Signaling) and anti-MCL-1 antibodies.

Thioflavin-T aggregation assay. Compounds **Q1**, **Q2**, control compound **9a,** and 2-10 μL DMSO (as negative control) were separately added to α-Synuclein disease-associated mutant A53T in buffer (100 mM HEPES, pH 7.4, 150 mM NaCl, 10% glycerol, 0.1% BOG and 5 μM Thioflavin-T) to reach a final compound concentration of 100 μM (2 μM for compounds **9a**), protein concentration of 200 nM in 100 μL system. The reaction was incubated at 37°C with frequent agitation. ThT fluorescence (excitation wavelength 440 nm, emission wavelength 482 nm, cutoff wavelength 475 nm) was measured with a FlexStation2 (Molecular Devices, Sunnyvale, CA, USA) at 37°C at 1 hour intervals for 30 hours.

Circular Dichroism (CD) Thermal Denaturation Study. The process of thermal denaturation of alpha-synuclein with and without compounds was monitored as the CD signal at 222 nm on BioLogic MOS-450 spectrophotometer equipped with a Peltier temperature controller, using a 1-cm pathlength quartz cuvette. DMSO solvent, compound Q1, Q2 were separately added into protein samples (0.05 mg/mL, 100 mL HEPES, 150 mM NaCl, 10%

glycerol, 0.1% BOG, 1% taurodeoxycholic acid) to a final concentration of 1 uM with 1% DMSO. Heating range was from 25°C to 60°Cat the rate of 1°C/min.

Scheme S1. Solid phase synthesis of trisubstituted triazine-piperazine-triazine scaffold **9**.

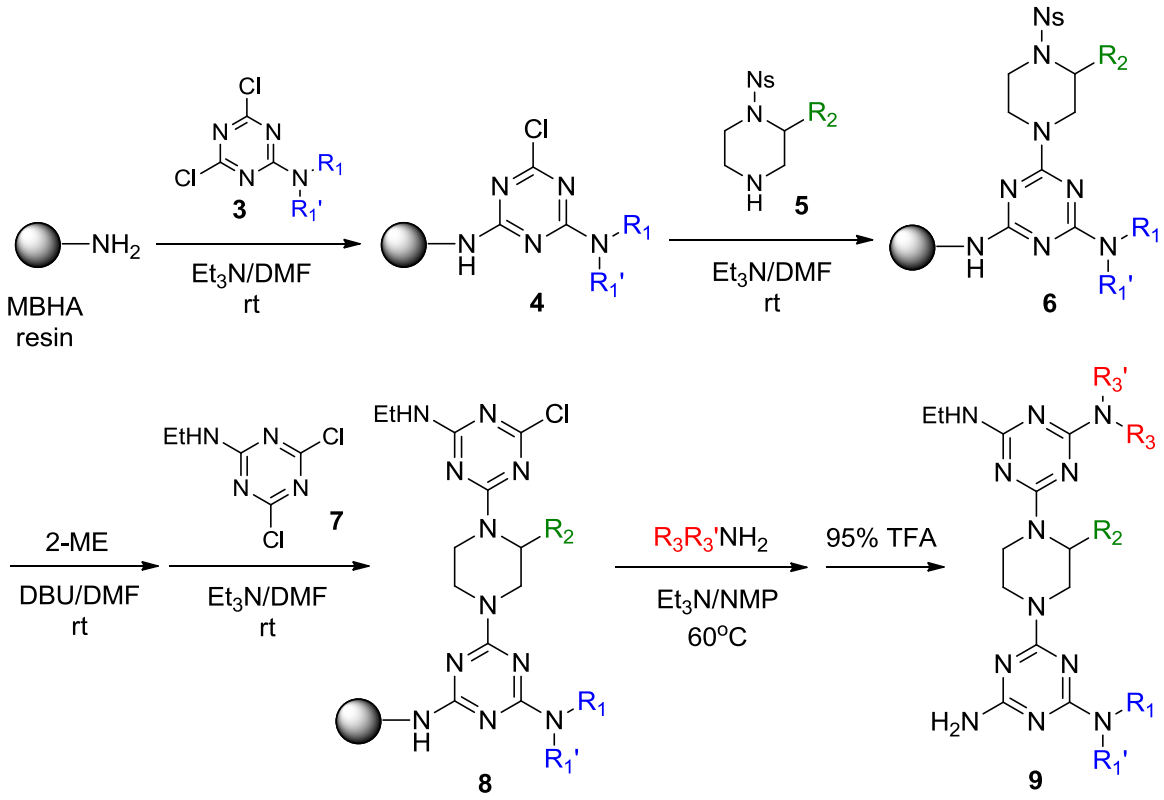

Figure S1. Mass and purity data of crude final products.

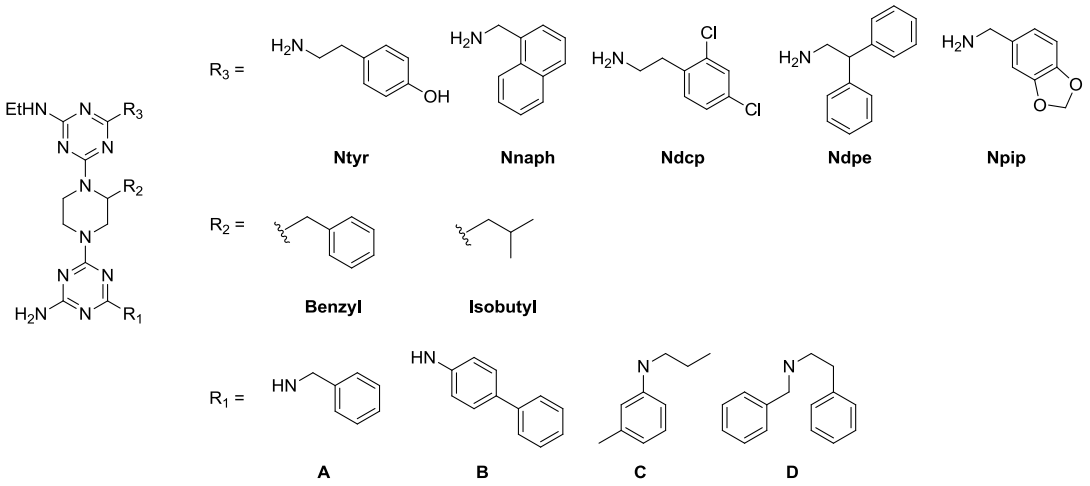

Entry	R_1	R_2	R_3	Calculated Mass (M)	Observed Mass (M+H)	Purity (%)
1	A	Benzyl	Ntyr	632.3	633.2	94
2	B	Benzyl	Ntyr	694.4	695.2	94
3	C	Benzyl	Ntyr	674.4	675.2	95
4	D	Benzyl	Ntyr	736.4	737.0	95
5	A	Benzyl	Nnaph	652.4	653.2	96
6	B	Benzyl	Nnaph	714.4	715.2	94
7	C	Benzyl	Nnaph	632.4	633.2	95
8	D	Benzyl	Nnaph	756.4	757.2	95
9	A	Benzyl	Ndcp	684.3	685.0	92
10	B	Benzyl	Ndcp	746.3	747.0	96
11	C	Benzyl	Ndcp	726.3	727.0	95
12	D	Benzyl	Ndcp	788.3	789.0	92
13	A	Benzyl	Ndpe	692.4	693.2	95
14	B	Benzyl	Ndpe	754.4	755.2	93
15	C	Benzyl	Ndpe	734.4	735.2	96
16	D	Benzyl	Ndpe	796.4	797.2	95
17	A	Benzyl	Npip	646.3	647.0	93
18	B	Benzyl	Npip	708.3	709.0	95
19	C	Benzyl	Npip	688.4	689.2	95
20	D	Benzyl	Npip	750.4	751.2	96

Figure S1. (Cont'd).

Entry	R_1	R_2	R_3	Calculated Mass (M)	Observed Mass (M+H)	Purity (%)
21	A	Isobutyl	Ntyr	598.4	599.2	98
22	B	Isobutyl	Ntyr	660.4	661.2	97
23	C	Isobutyl	Ntyr	640.4	641.2	97
24	D	Isobutyl	Ntyr	702.4	703.2	98
25	A	Isobutyl	Nnaph	618.4	619.2	94
26	B	Isobutyl	Nnaph	680.4	681.2	97
27	C	Isobutyl	Nnaph	660.4	661.2	96
28	D	Isobutyl	Nnaph	722.4	723.2	95
29	A	Isobutyl	Ndcp	650.3	651.0	94
30	B	Isobutyl	Ndcp	712.3	713.0	97
31	C	Isobutyl	Ndcp	692.3	693.0	96
32	D	Isobutyl	Ndcp	754.4	755.2	96
33	A	Isobutyl	Ndpe	658.4	659.2	96
34	B	Isobutyl	Ndpe	720.4	721.2	97
35	C	Isobutyl	Ndpe	700.4	701.2	96
36	D	Isobutyl	Ndpe	762.5	763.2	95
37	A	Isobutyl	Npip	612.3	613.0	93
38	B	Isobutyl	Npip	674.4	675.2	95
39	C	Isobutyl	Npip	654.4	655.2	96
40	D	Isobutyl	Npip	716.4	717.2	95
Average purity						92.2%

Figure S2. LC/MS data of representative crude products.

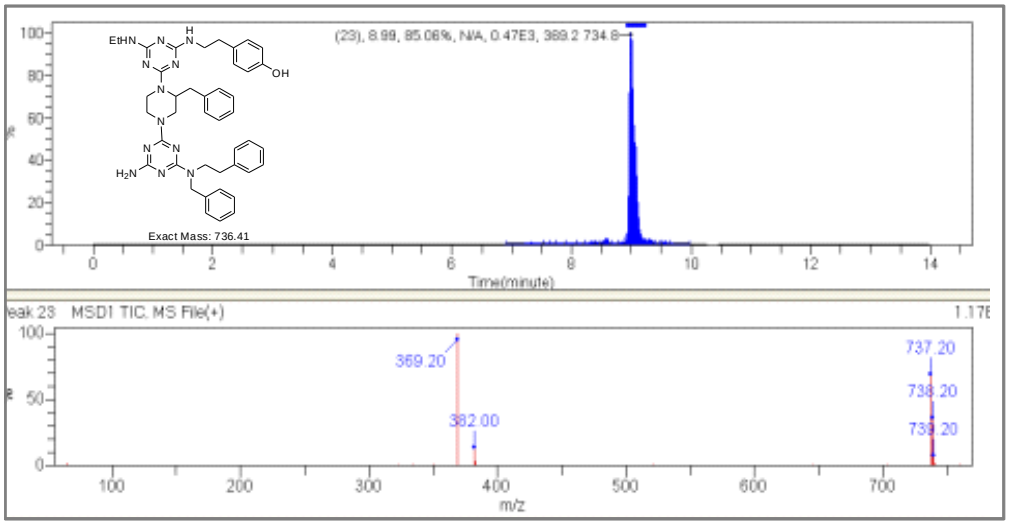

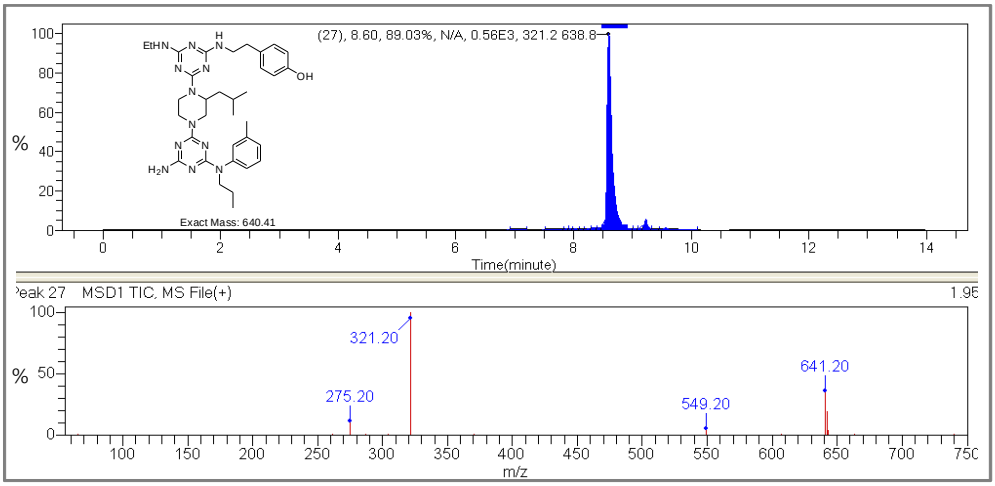

Figure S3. Synthesis of a peptoid-encoded OBOC combinatorial library of triazine-piperazine-triazines.

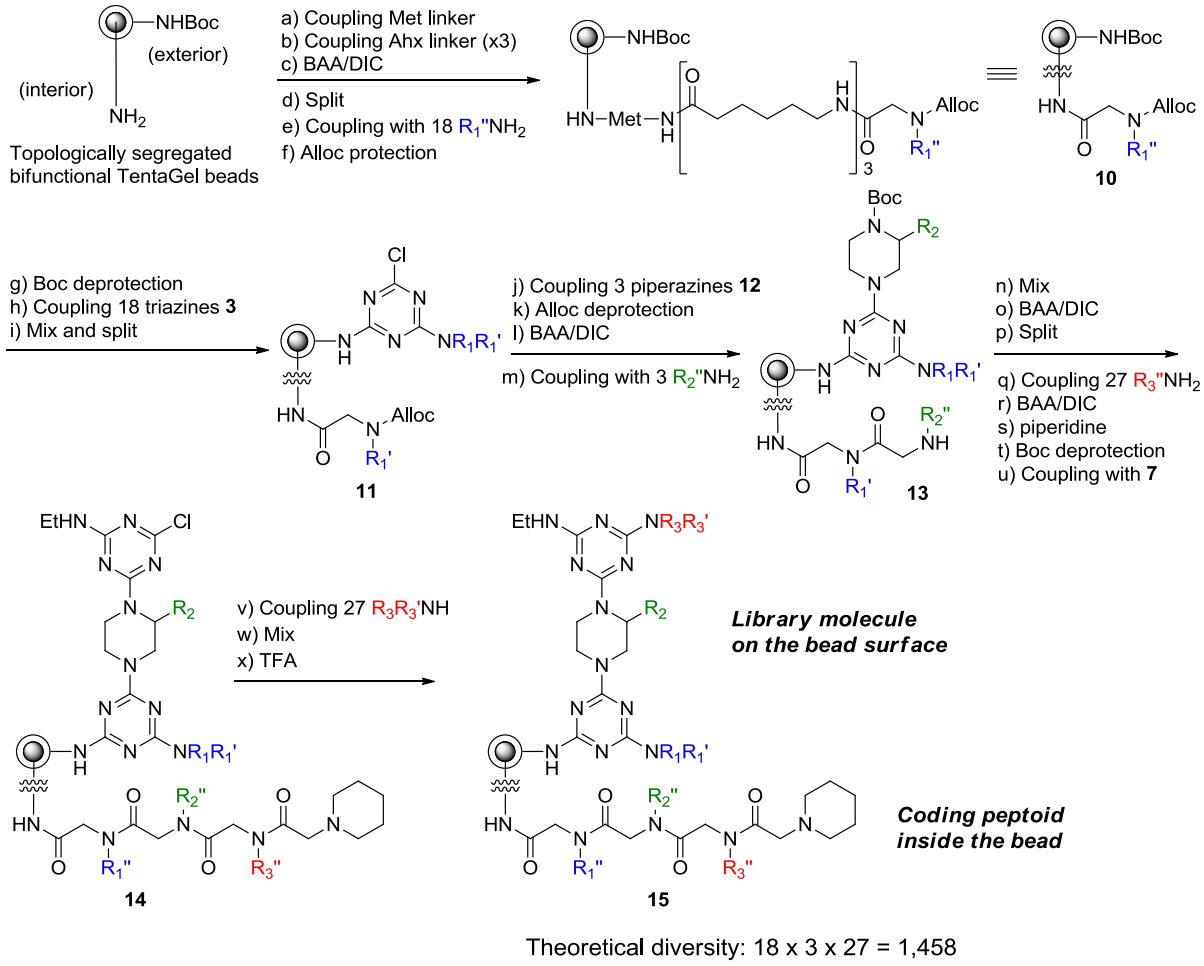

Figure S4. Chemical structures of building blocks used for library synthesis. The structures in parenthesis are amines used for coding peptoid synthesis when building blocks are not identical.

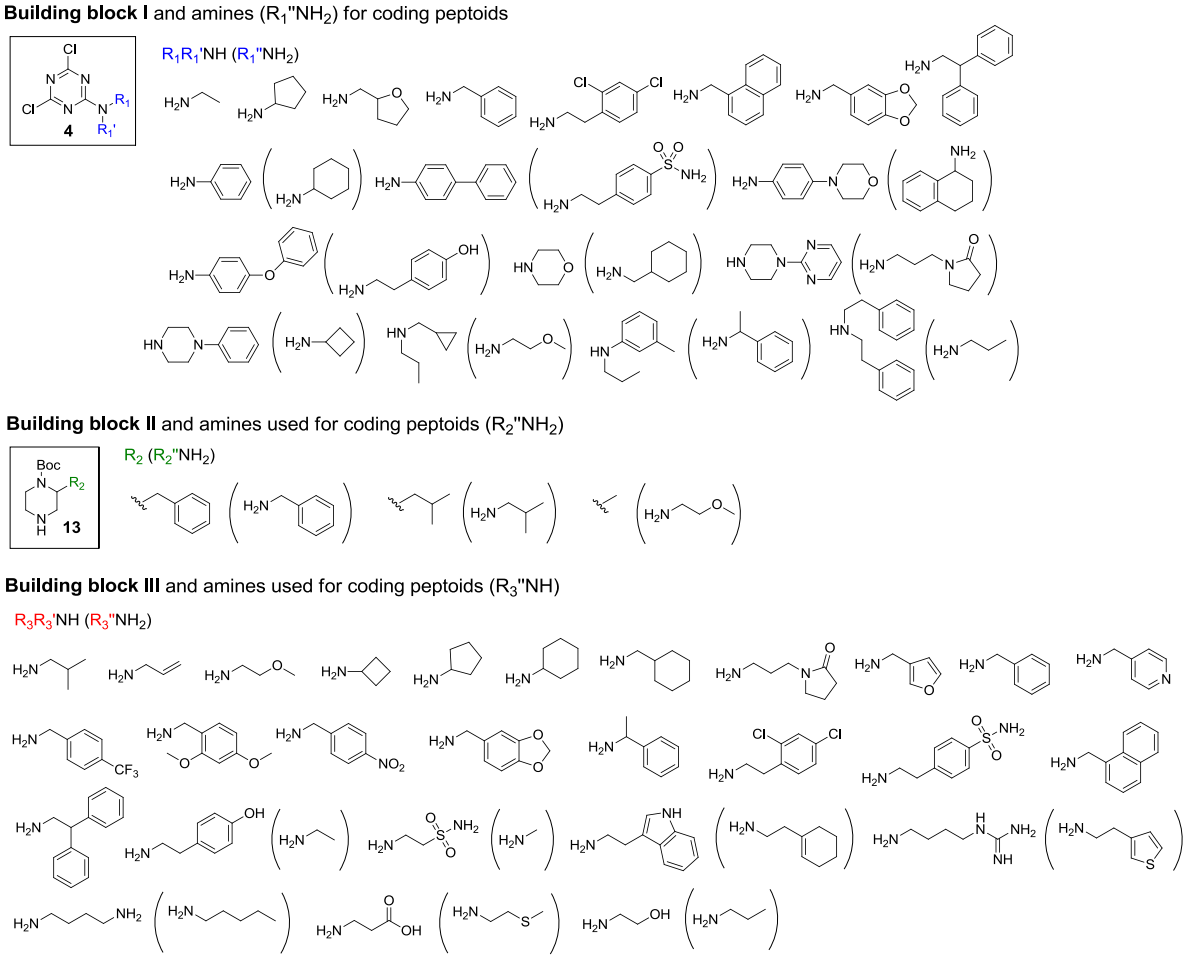

Figure S5. MS and MS/MS data of coding peptoids.

Peptoid 1 (Chemical formula: $C_{57}H_{78}N_8O_{11}$, Exact mass: 1050.58)

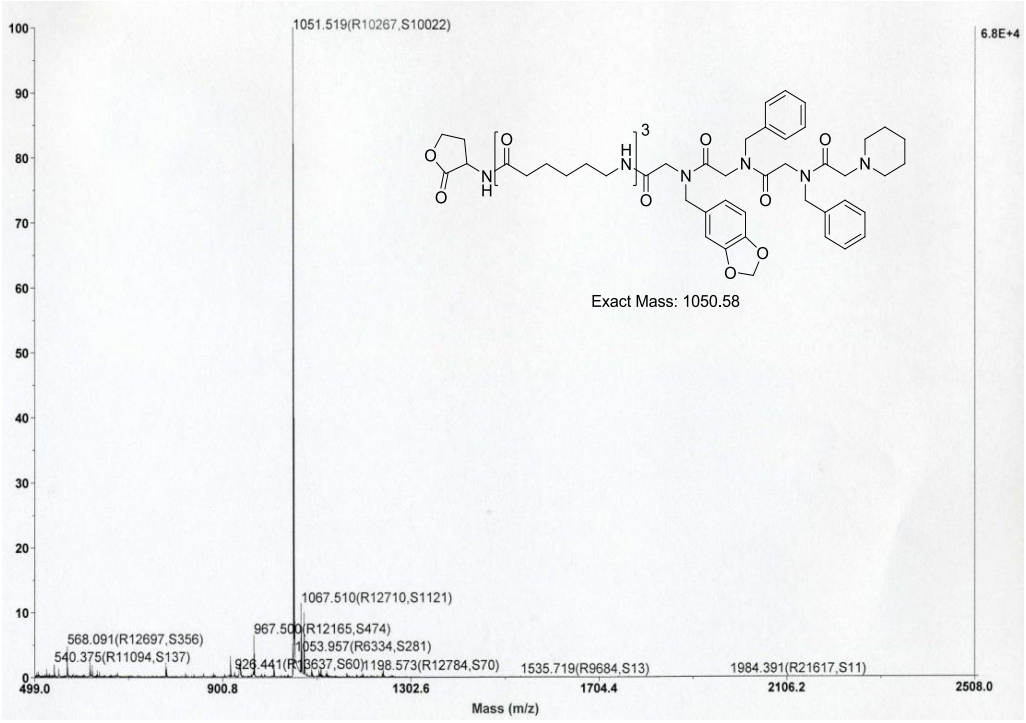

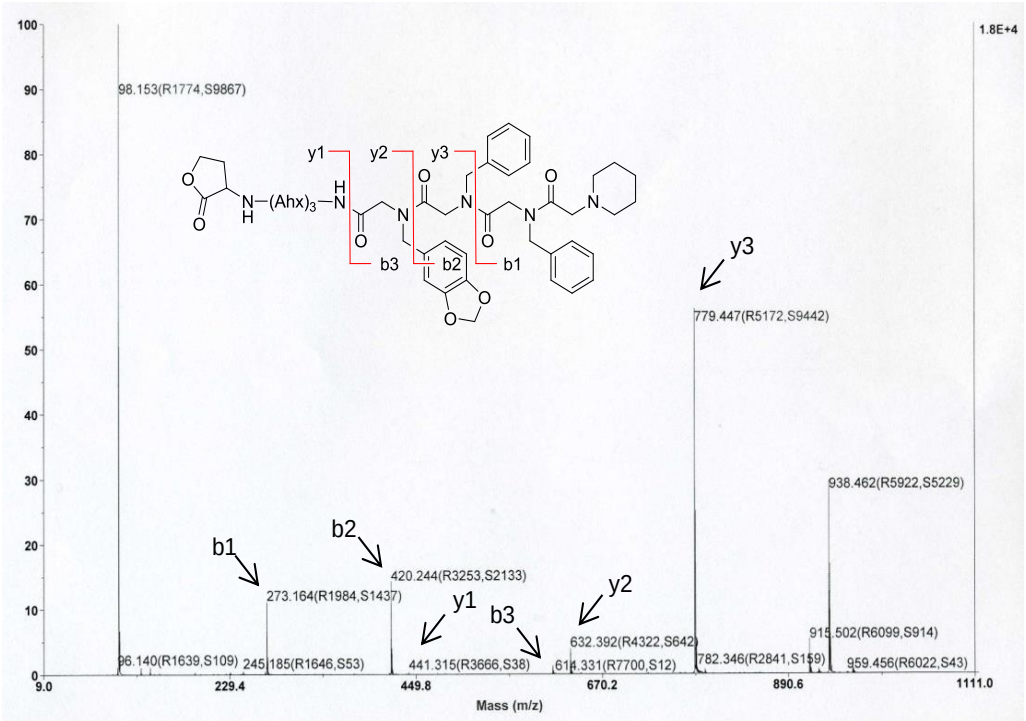

Figure S5. (Cont'd)

Peptoid 2 (Chemical formula: $C_{53}H_{78}N_8O_{12}$, Exact mass: 1018.57)

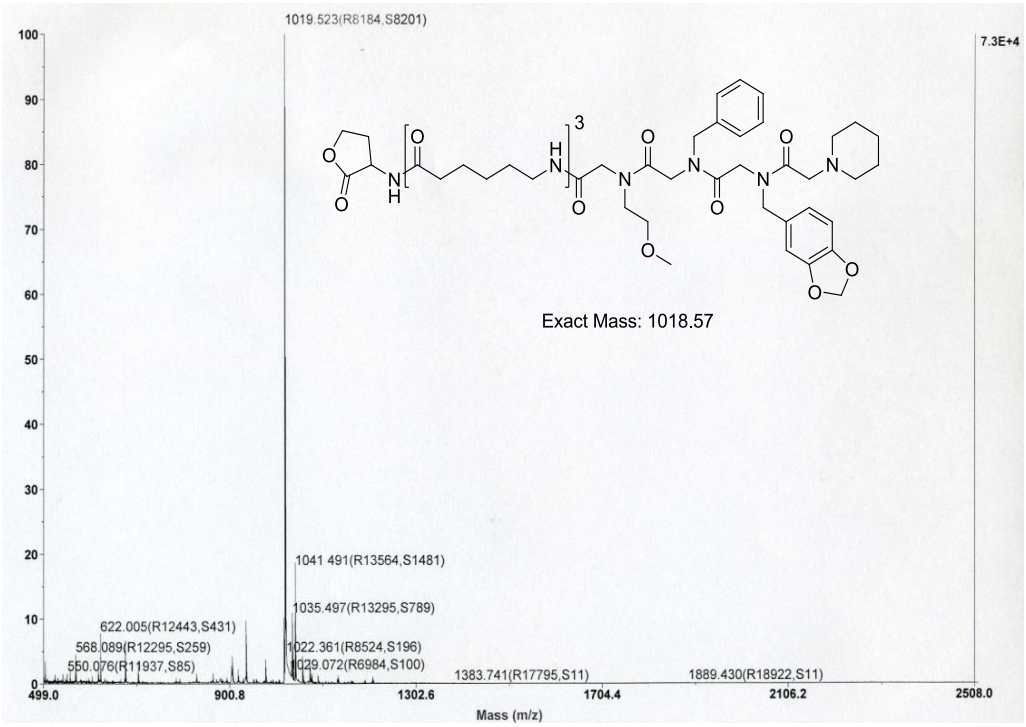

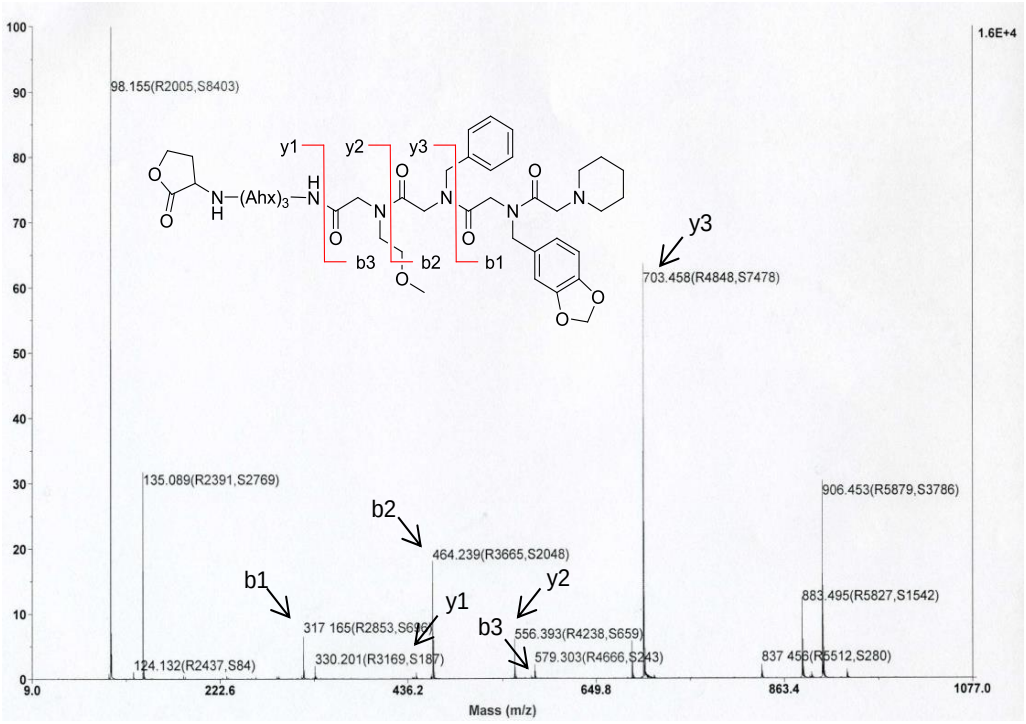

Figure S5. (Cont'd)

Peptoid 3 (Chemical formula: $C_{52}H_{78}N_8O_{10}$, Exact mass: 974.58)

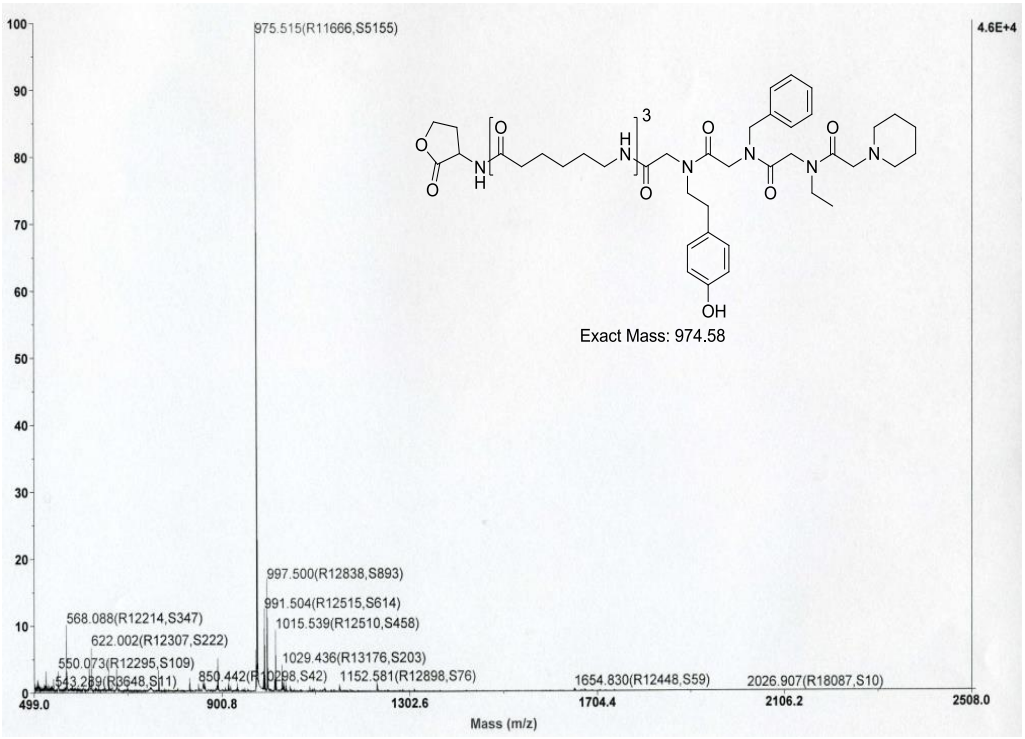

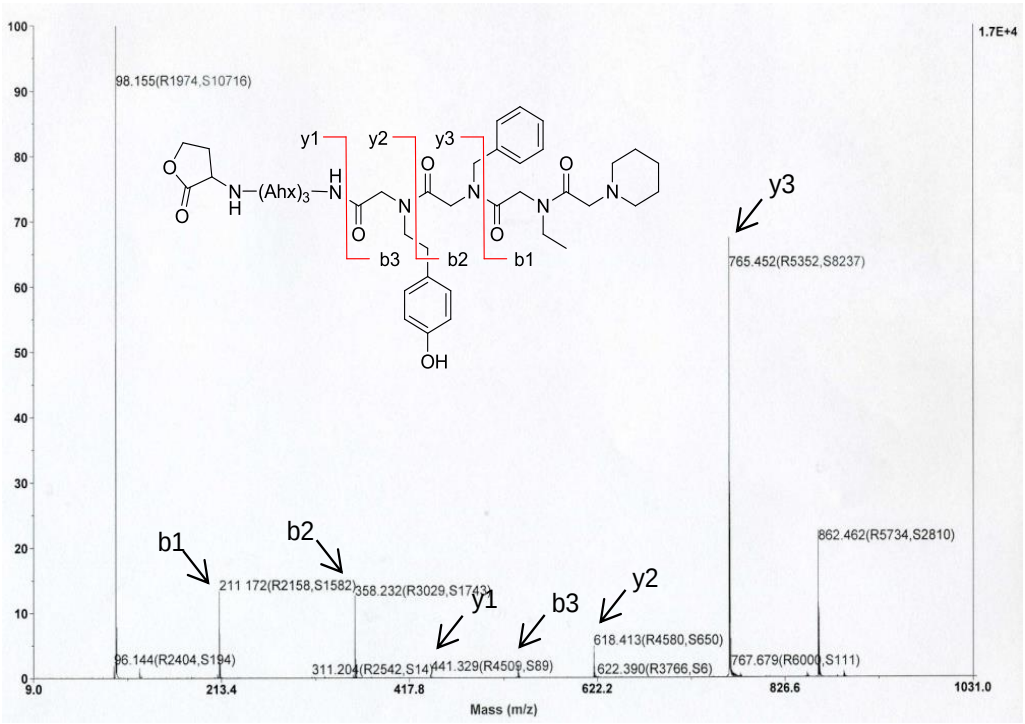

Figure S6. Peptoid sequence of hit beads and the corresponding structures.

Entry	Peptoid sequence	Number of hit beads	Structure of hit compounds
1	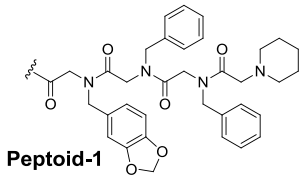 Peptoid-1	5	**9a**
2	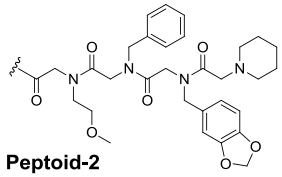 Peptoid-2	3	**9b**
3	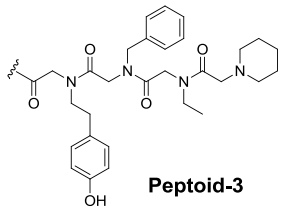 Peptoid-3	2	**9c**

Figure S7. Synthesis of fluorescently-labeled hit compounds **9a-c-FL** and **FL-linker**.

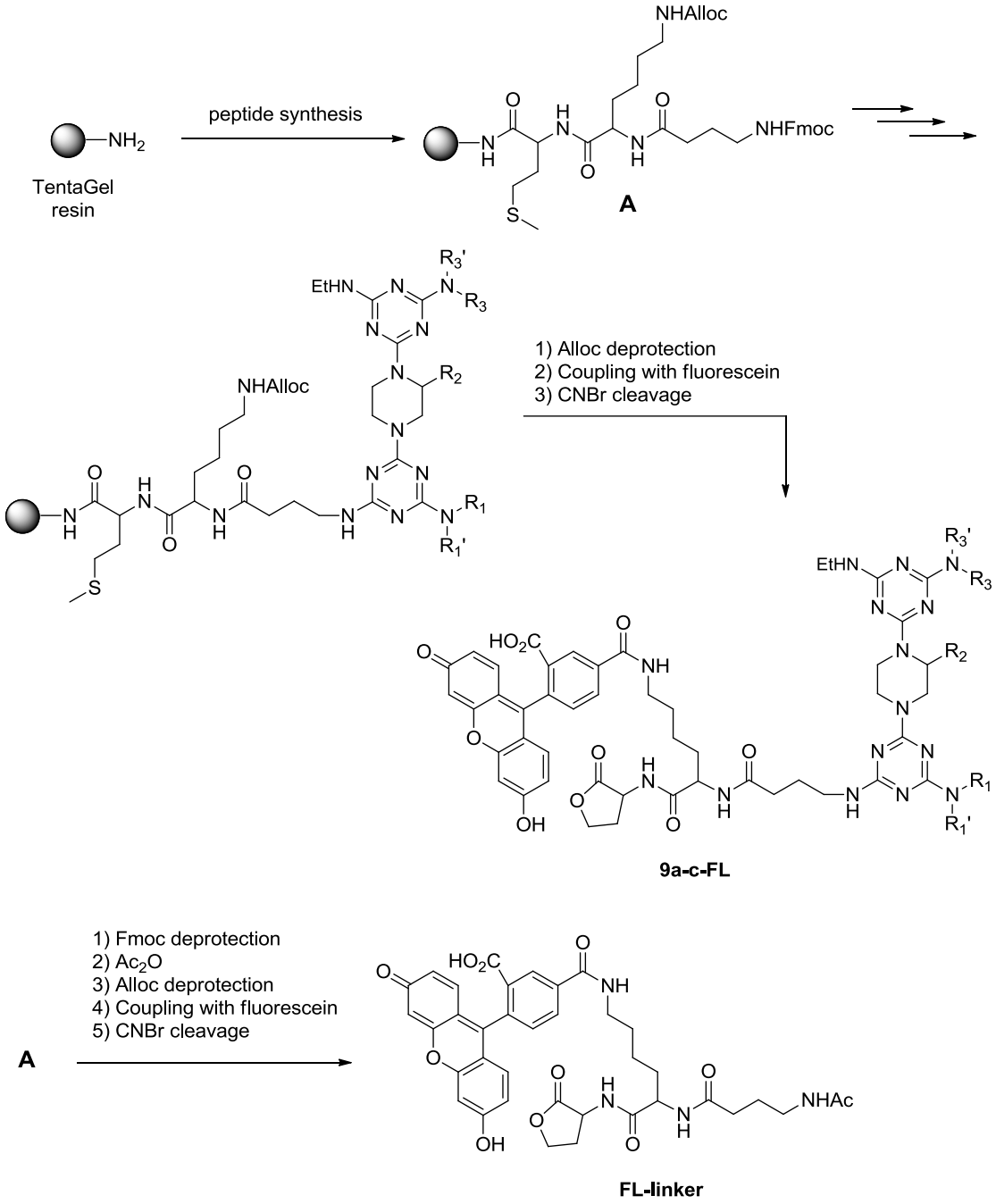

Figure S8. MALDI-TOF Mass spectra of **9a-c-FL**.

9a-FL

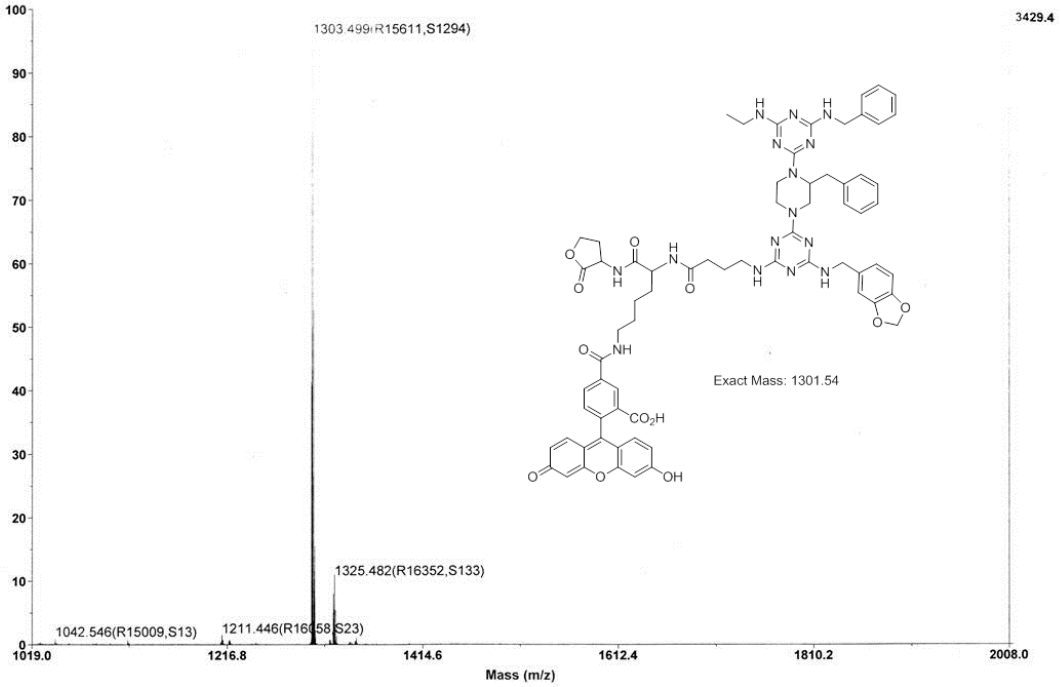

Figure S8. (Cont'd)

9b-FL

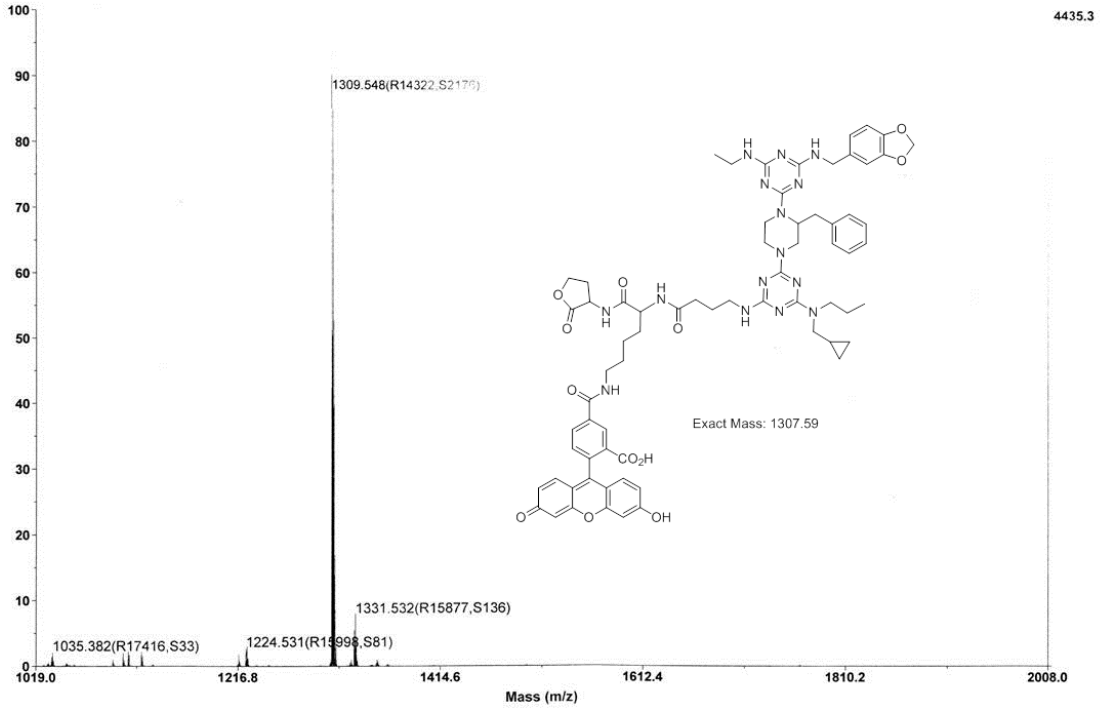

Figure S8. (Cont'd)

9c-FL

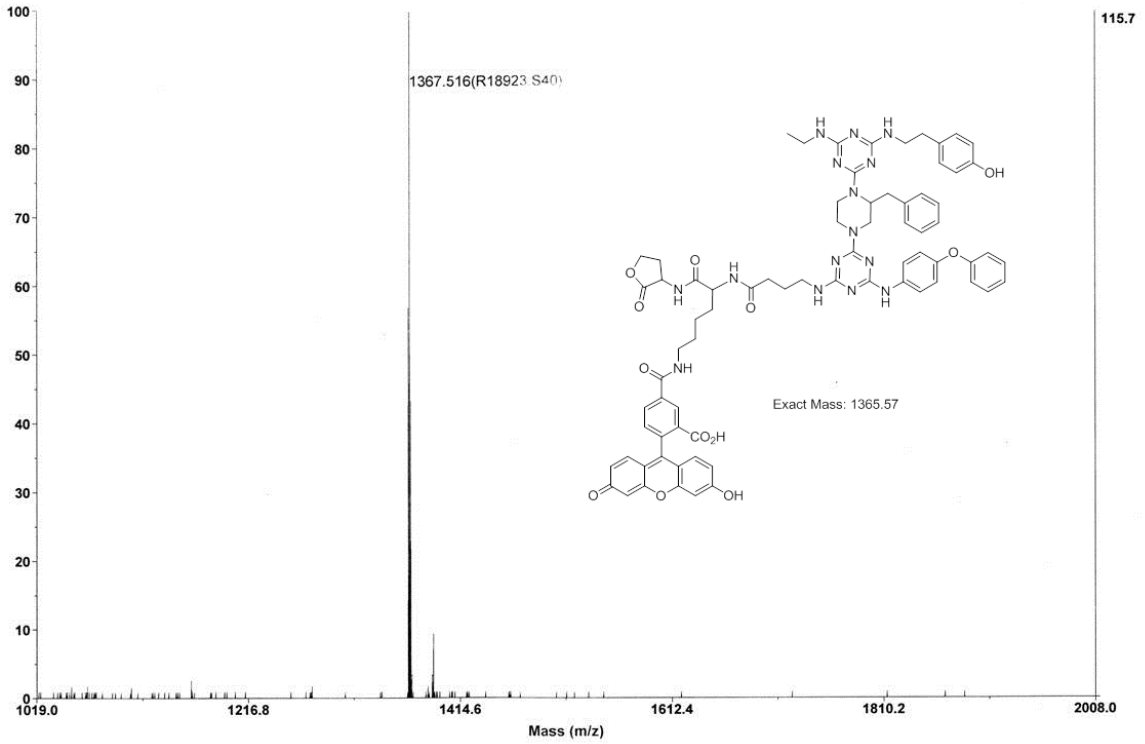

Figure S9. LC/MS data for **9a-c**, **9-nc**, **Q1-2**, and **FL-linker**.

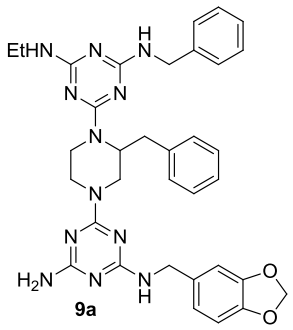

Calculated Mass: 646.32

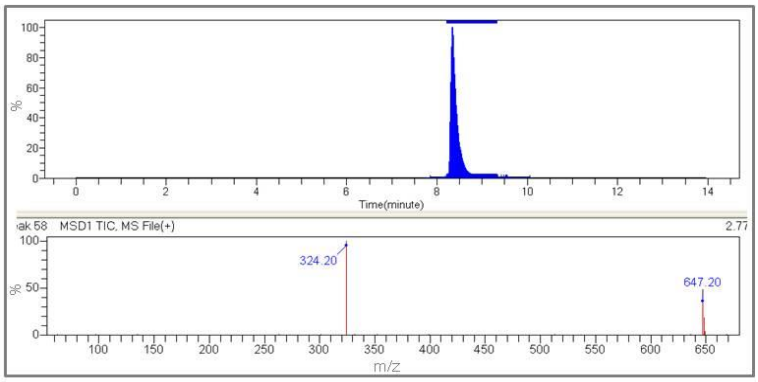

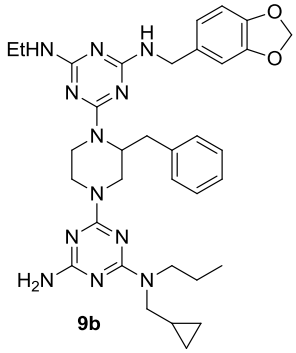

Calculated Mass: 652.37

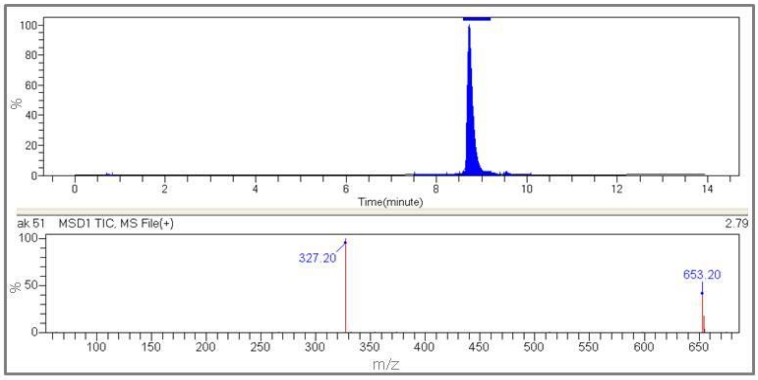

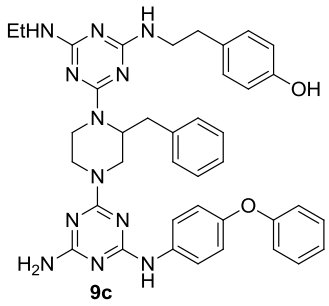

Calculated Mass: 710.36

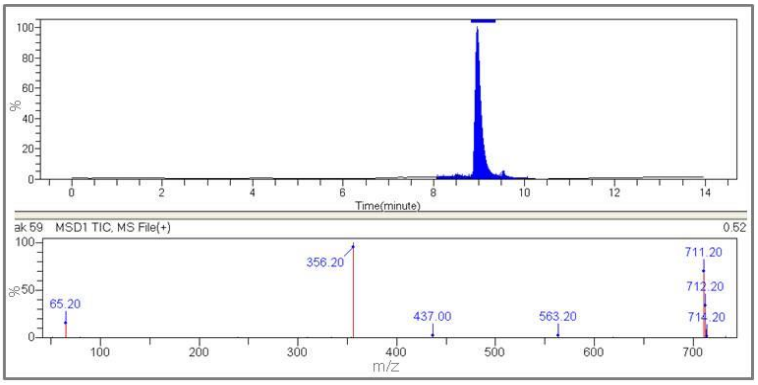

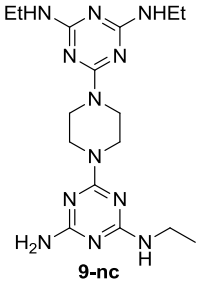

Calculated Mass: 388.26

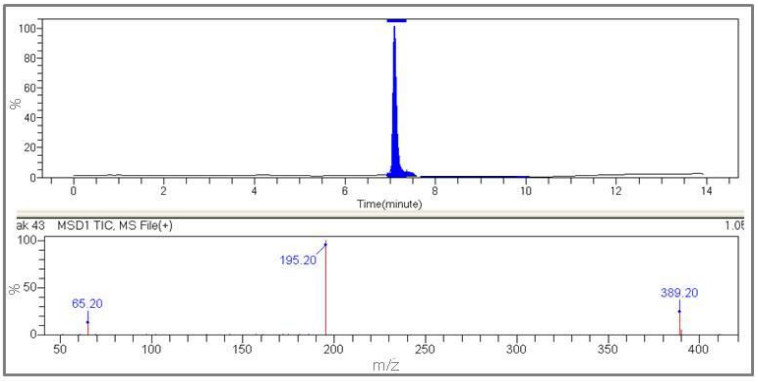

Figure S9. (Cont'd)

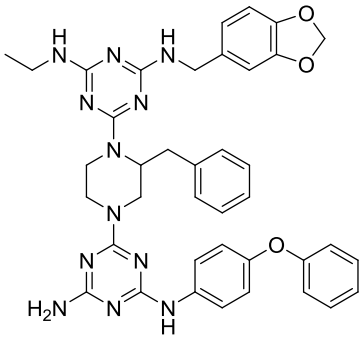

Q1 Exact Mass: 724.33

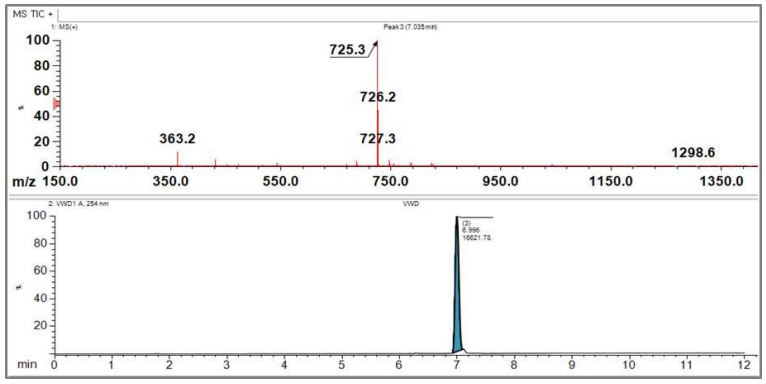

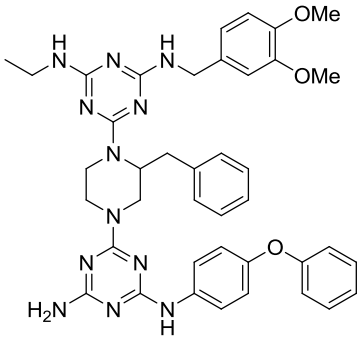

Q2 Exact Mass: 740.37

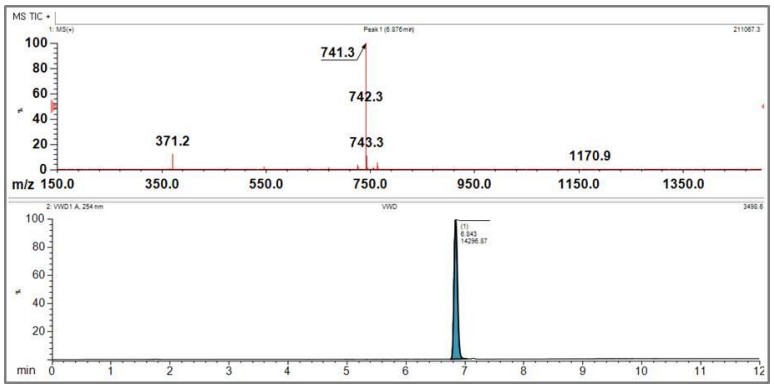

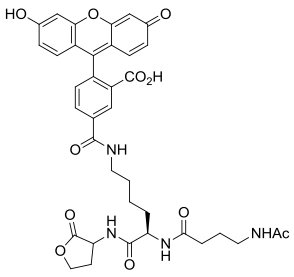

Exact Mass: 714.25

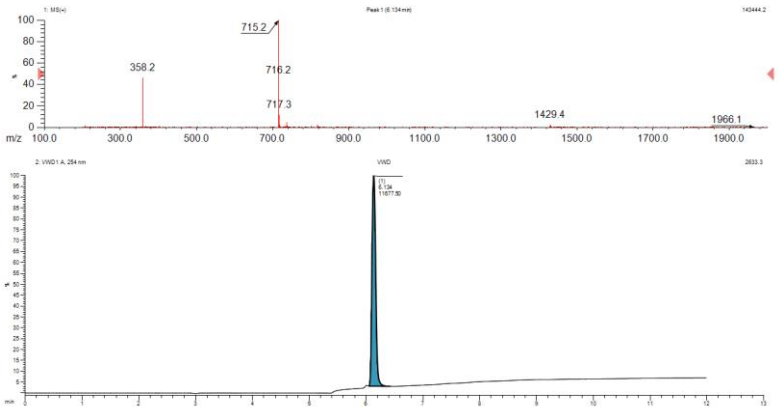

FL-linker

Figure S10. Inhibition curves of **9c** and a BH3 peptide for fluorescein-labeled BH3 peptide binding to BCL-XLΔC. Error bars represent standard deviation from two independent experiments.

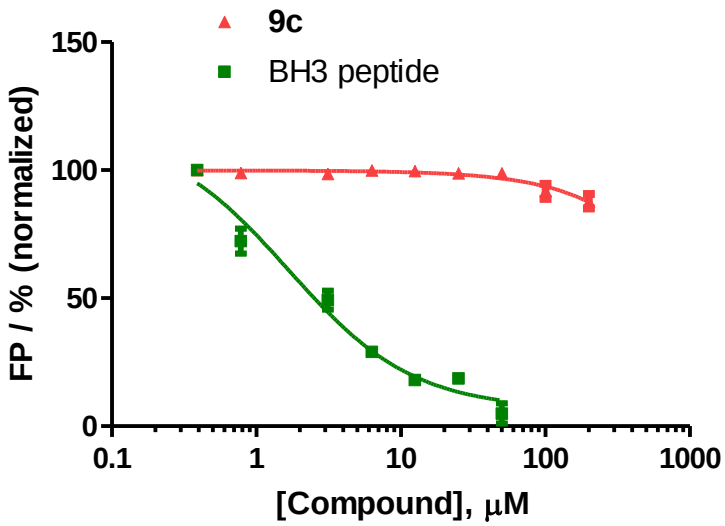

Figure S11. Predicted binding mode of **9c** on MCL-1. (A) Crystal structure of BH3 peptide in complex with MCL-1ΔNΔC (PDB ID: 3MK8). Side chains of three key hydrophobic residues (Leu213, Val216 and Val220) of BH3 peptide are shown with cartoon representation of the helix. (B) Predicted binding modes of **9c** in the binding sites of the MCL-1ΔNΔC.

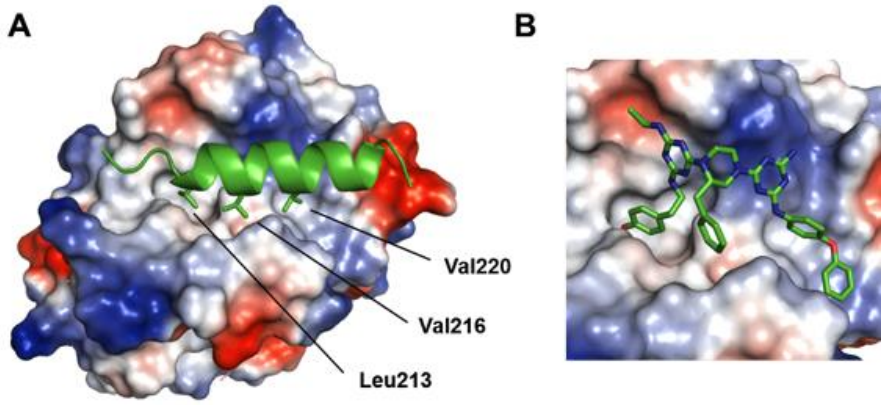

Figure S12. Co-immunoprecipitation assay. Jurkak T cells were treated with DMSO, **9c** or **9-nc** for 2.5 hr, immunoprecipitated by MCL-1 antibody and detected MCL-1 and BAK by western blot.

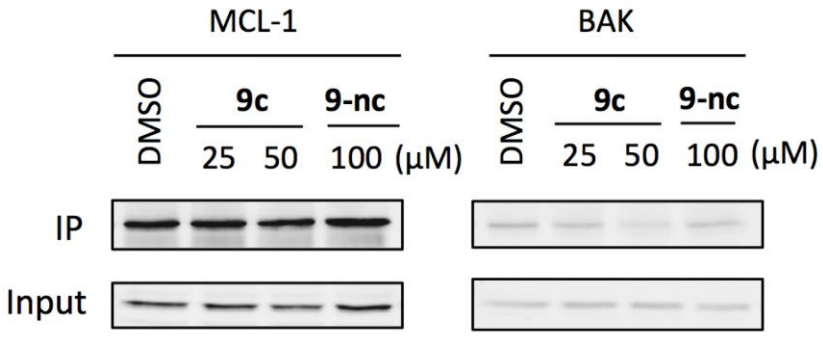

Figure S13. Cellular activity of **9c (**MCL-1 inhibitor) and **9-nc** (an MCL-1 negative control). (A) U266 cells were treated with varying concentrations of **9c** and **9-nc** for 24 hr. Cell viability was assessed by CellTiter MTS assay kit (Promega). **9c** decreases cell viability of human multiple myeloma U266 cells in a dose-dependent manner while **9-nc**, a negative control, has no effect. Error bars indicate standard deviation from two independent experiments. (B) **9c** and **9-nc** have little effect on cell viability of normal HEK293 cells. (C) Caspase assays with U266 cells and WS-1 cells. Cells were treated with DMSO or indicated concentrations of **9c** for 16 hr, and caspase activity was analyzed by Caspase-Glo 3/7 assay kit (Promega). Error bars represent standard deviation from three independent experiments.

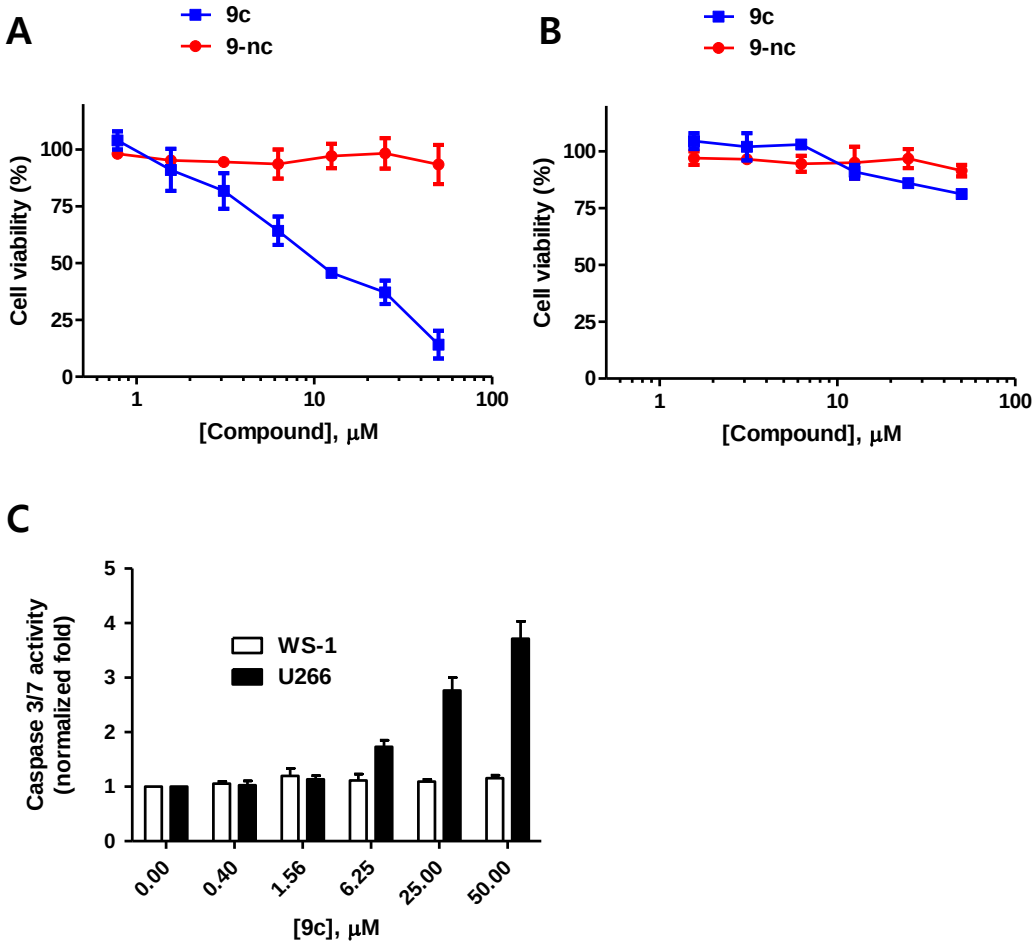

Figure S14. Construct of α-synuclein and its biotinylation. A polypeptide extension MKCK was inserted at the N-terminus of α-synuclein and used for covalent linkage with biotin for on-bead screening. N and C indicate the N- and C-terminus of α-synuclein, respectively.

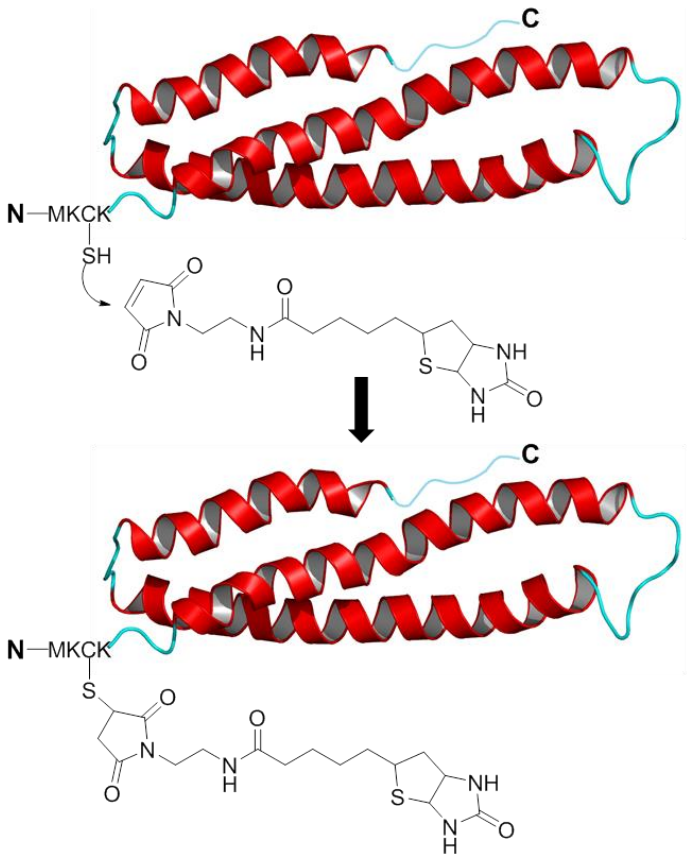

Figure S15. (A) Inhibition curves of **Q1**, **Q2** and a BH3 peptide for fluorescein-labeled BH3 peptide binding to MCL-1ΔNΔC. (B) The effect of **Q1** and **Q2** on cell viability of Jurkat T cells and U266 cells. Error bars represent standard deviation from two independent experiments**.**

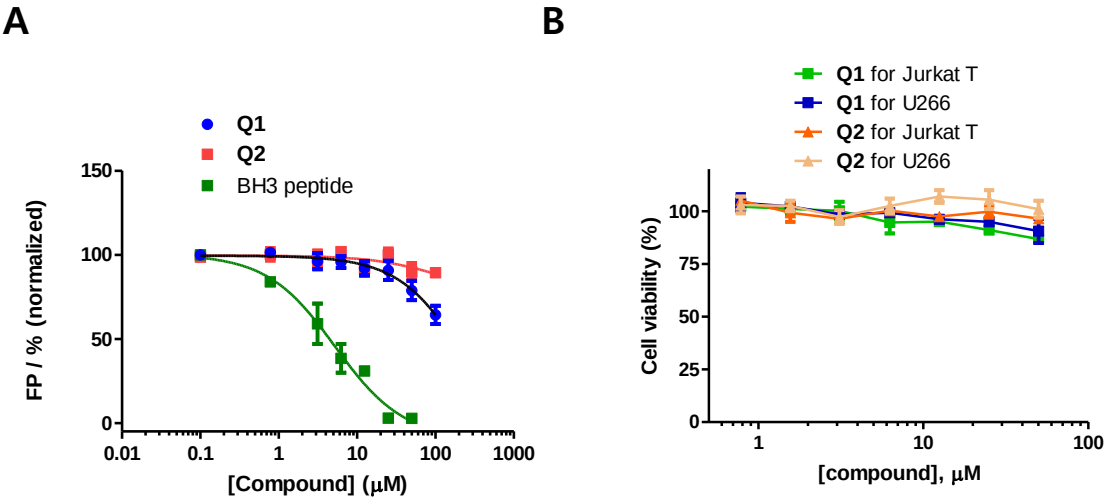

Figure S16. Thermal denaturation spectra of a-synuclein with or without **Q1** and **Q2**.

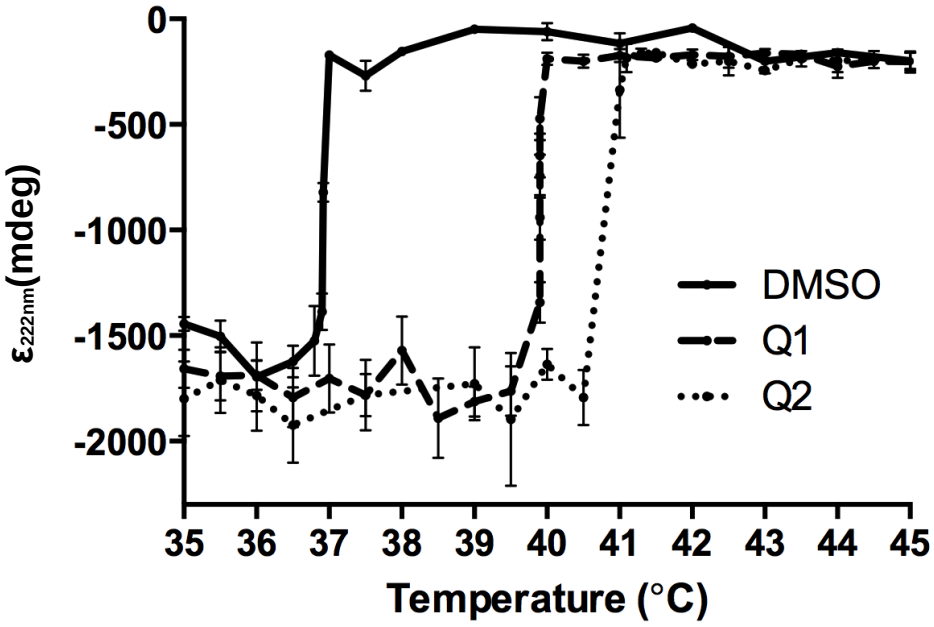

Figure S17. ^{1}H and ^{13}C NMR spectra for **9a-d**, **9-nc**, and **Q1-2**.

9a

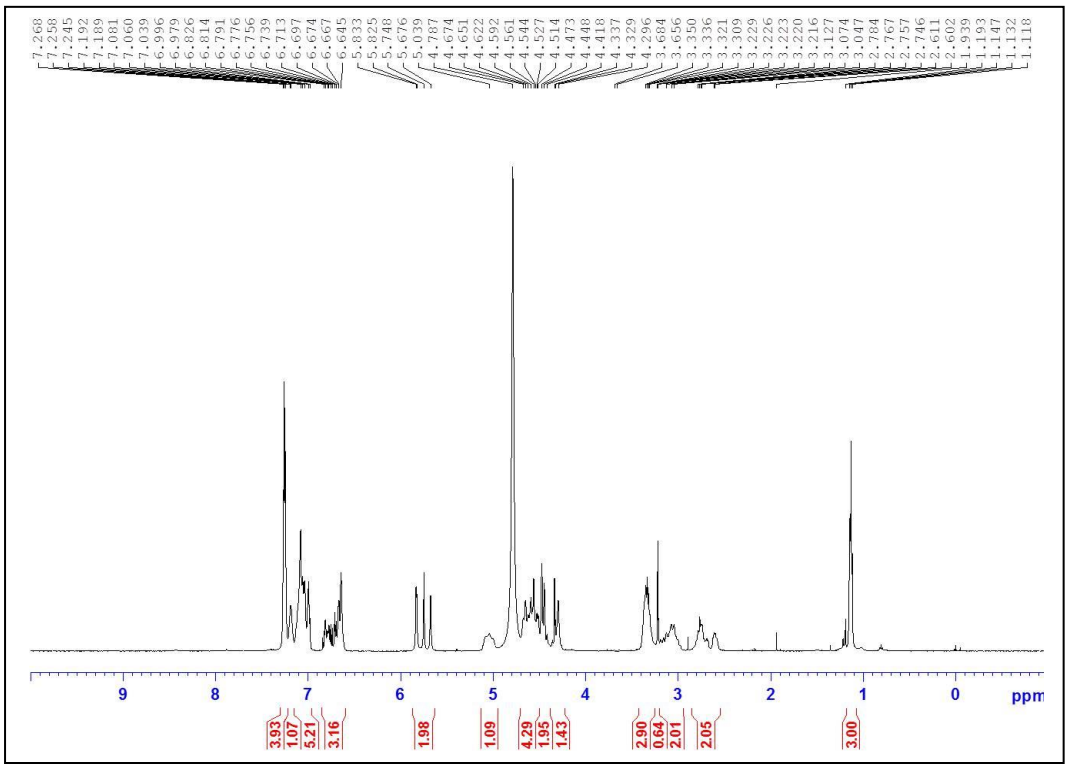

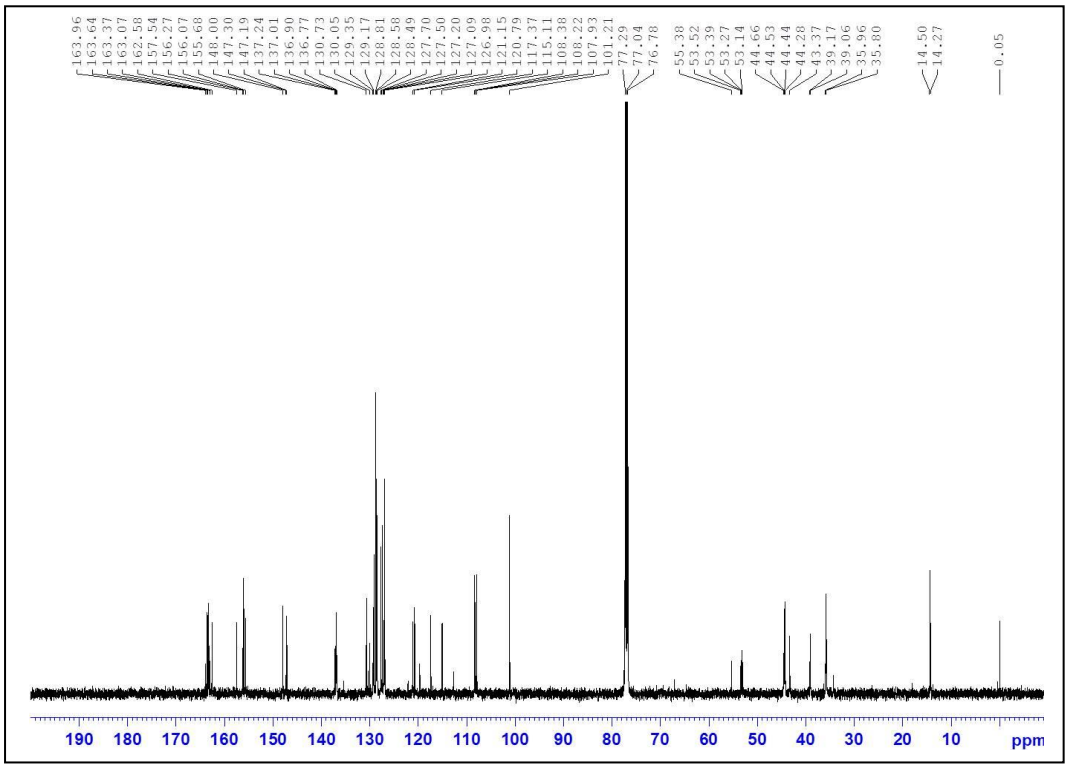

9b

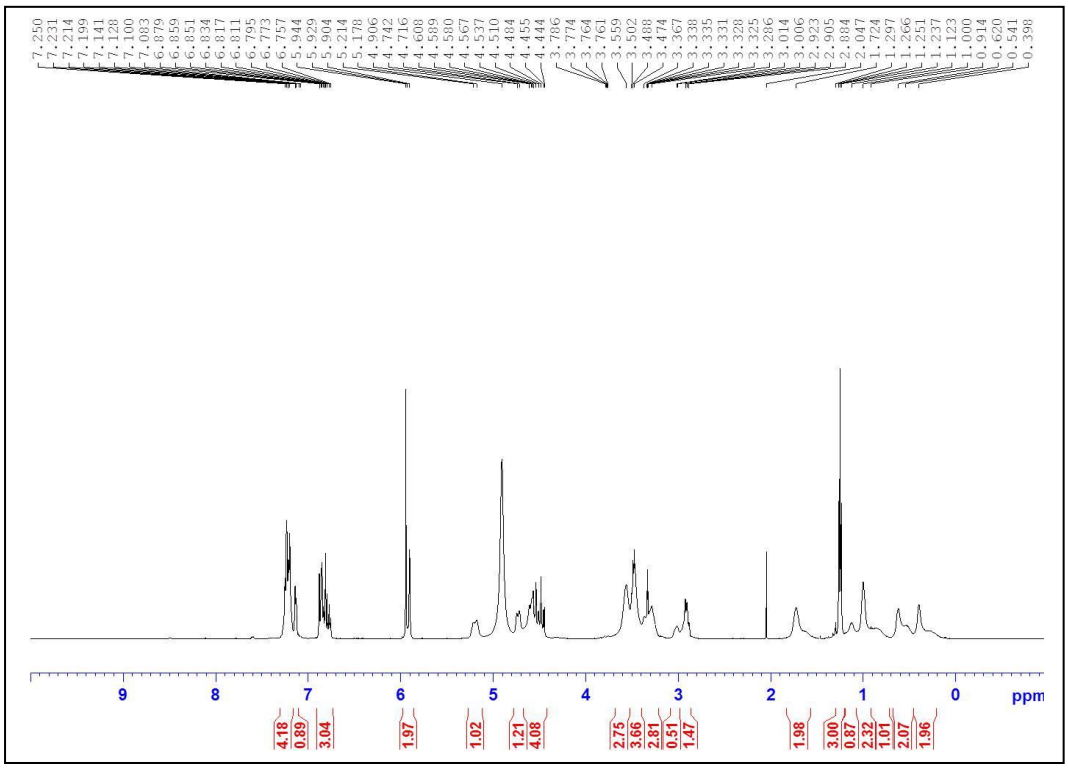
7.250
7.231
7.214
7.199
7.141
7.128
7.100
7.083
6.879
6.859
6.851
6.834
6.817
6.811
6.795
6.773
6.757
5.944
5.929
5.904
5.214
5.178
4.906
4.742
4.716
4.608
4.589
4.580
4.567
4.537
4.510
4.484
4.455
4.444
3.796
3.774
3.764
3.761
3.559
3.502
3.488
3.474
3.367
3.338
3.335
3.331
3.328
3.325
3.286
3.014
3.006
2.923
2.905
2.884
2.047
1.724
1.297
1.266
1.251
1.237
1.123
1.000
0.914
0.620
0.541
0.398
9
8
7
6
5
4
3
2
1
0
ppm
4.18
0.89
3.04
1.97
1.02
1.21
4.08
2.75
3.66
2.81
0.51
1.47
1.98
3.00
0.87
2.32
1.01
2.07
1.96

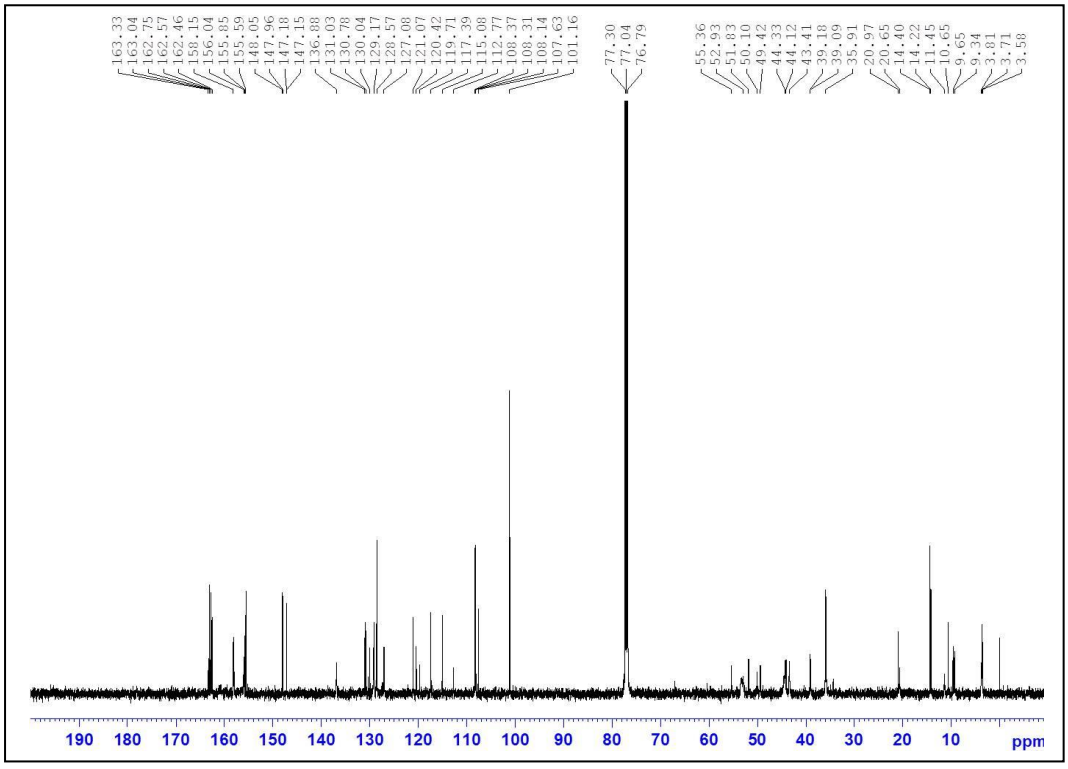
163.33
163.04
162.75
162.57
162.46
158.15
156.04
155.85
155.59
148.05
147.96
147.18
147.15
136.88
131.03
130.78
130.04
129.17
128.57
127.08
121.07
120.42
119.71
117.39
115.08
112.77
108.37
108.31
108.14
107.63
101.16
77.30
77.04
76.79
55.36
52.93
51.83
50.10
49.42
44.33
44.12
43.41
39.18
39.09
35.91
20.97
20.65
14.40
14.22
11.45
10.65
9.65
9.34
3.81
3.71
3.58
190
180
170
160
150
140
130
120
110
100
90
80
70
60
50
40
30
20
10
ppm

9c

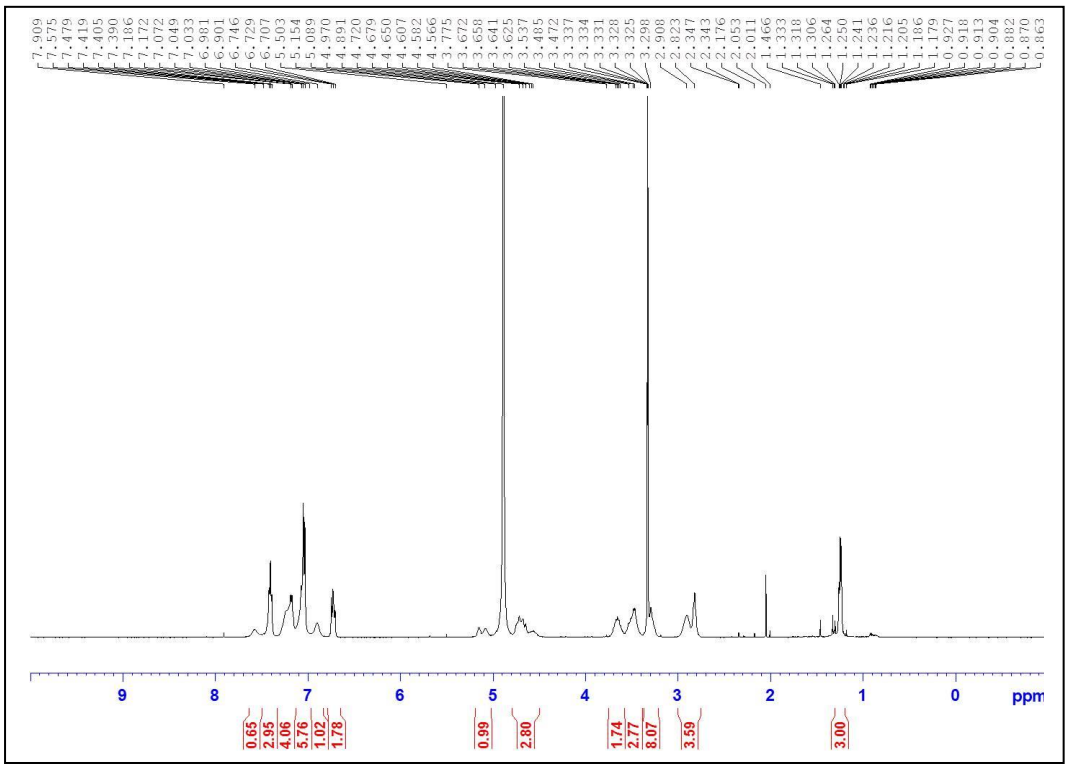

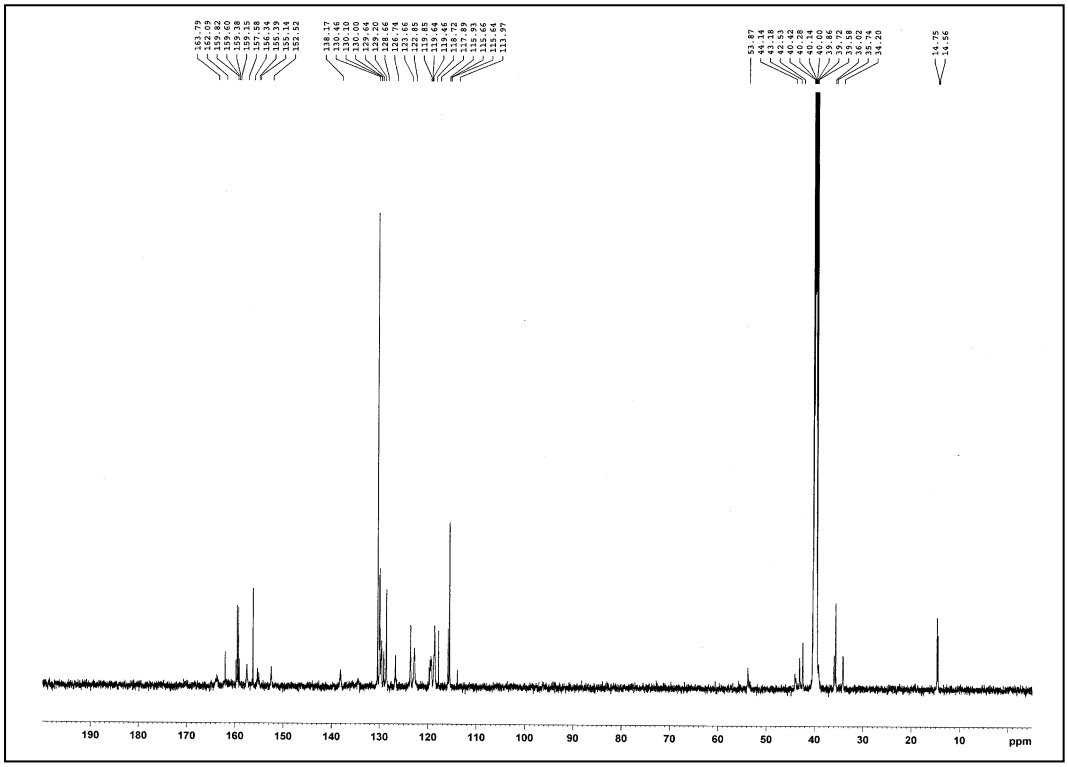

9-nc

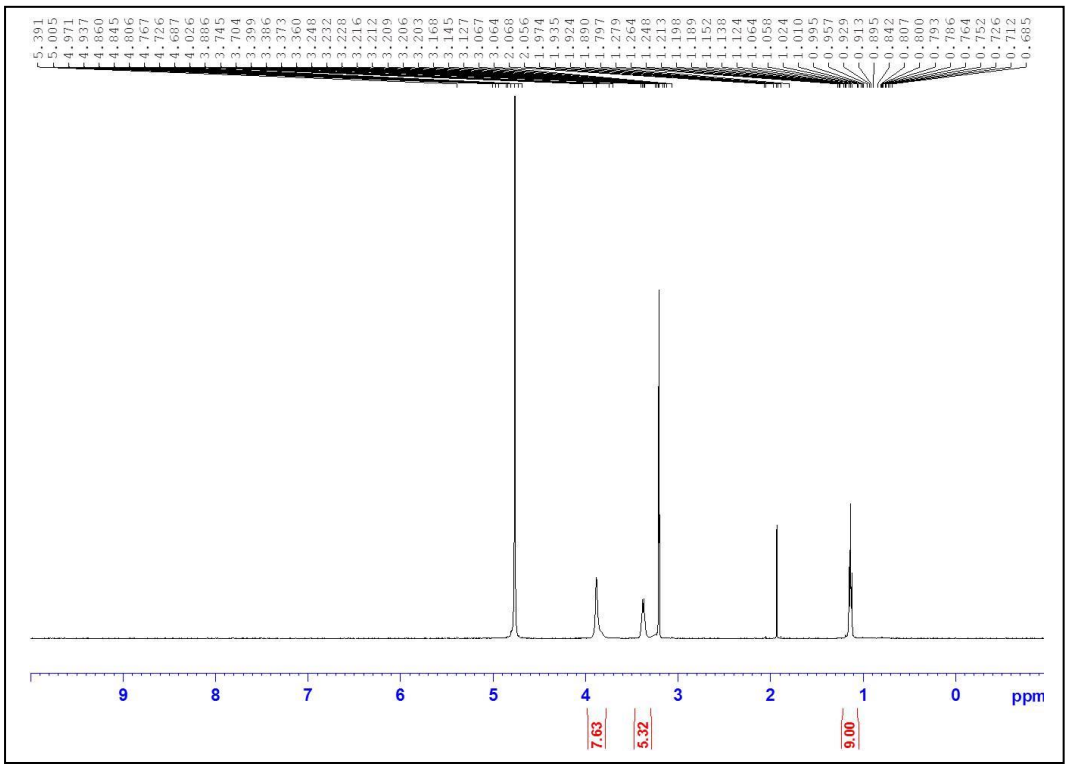
9
8
7
6
5
4
3
2
1
0
ppm
7.63
5.32
9.00

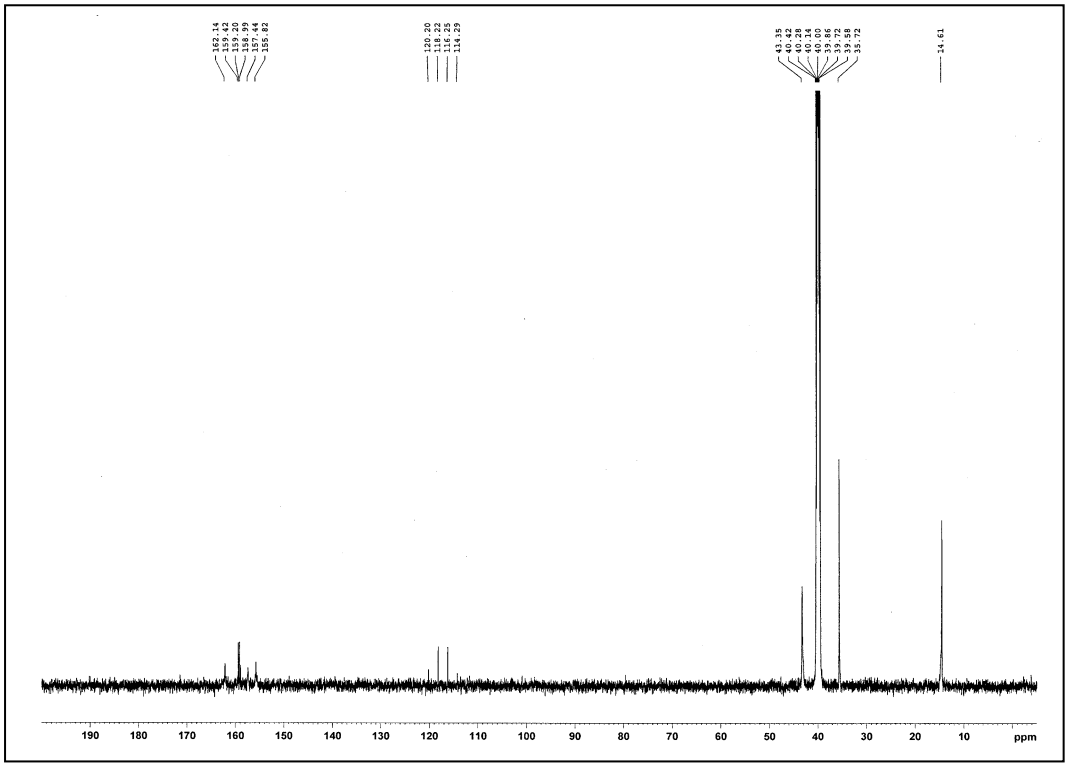
190
180
170
160
150
140
130
120
110
100
90
80
70
60
50
40
30
20
10
ppm

Q1

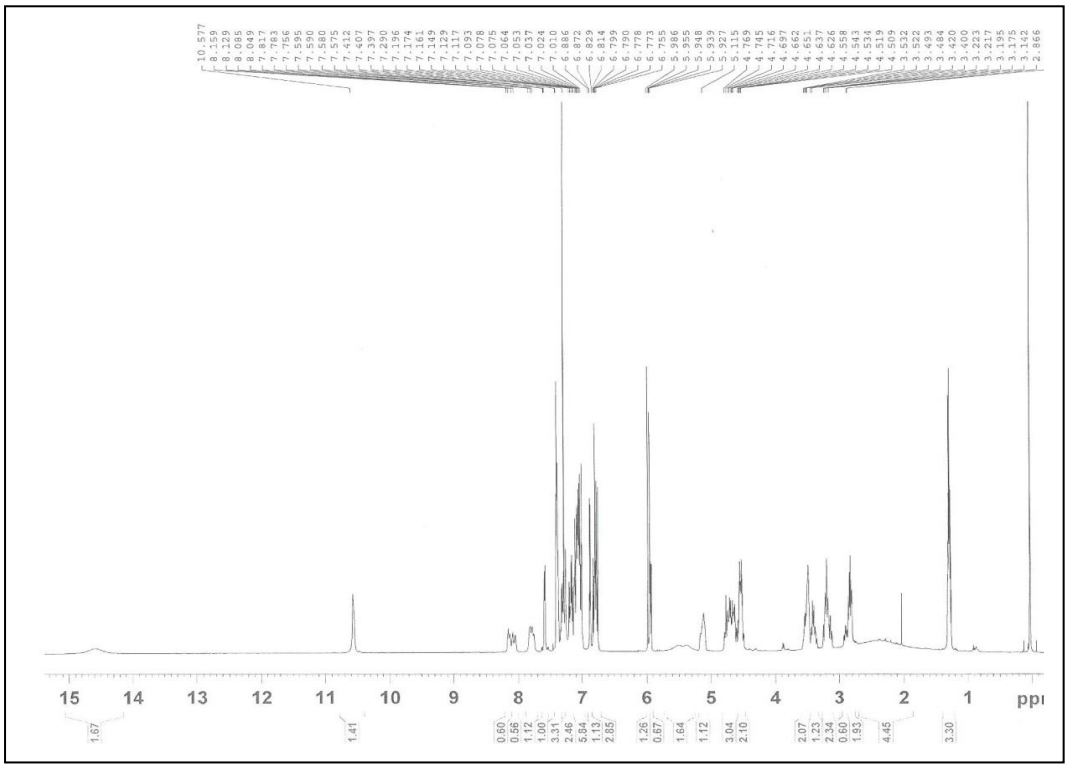

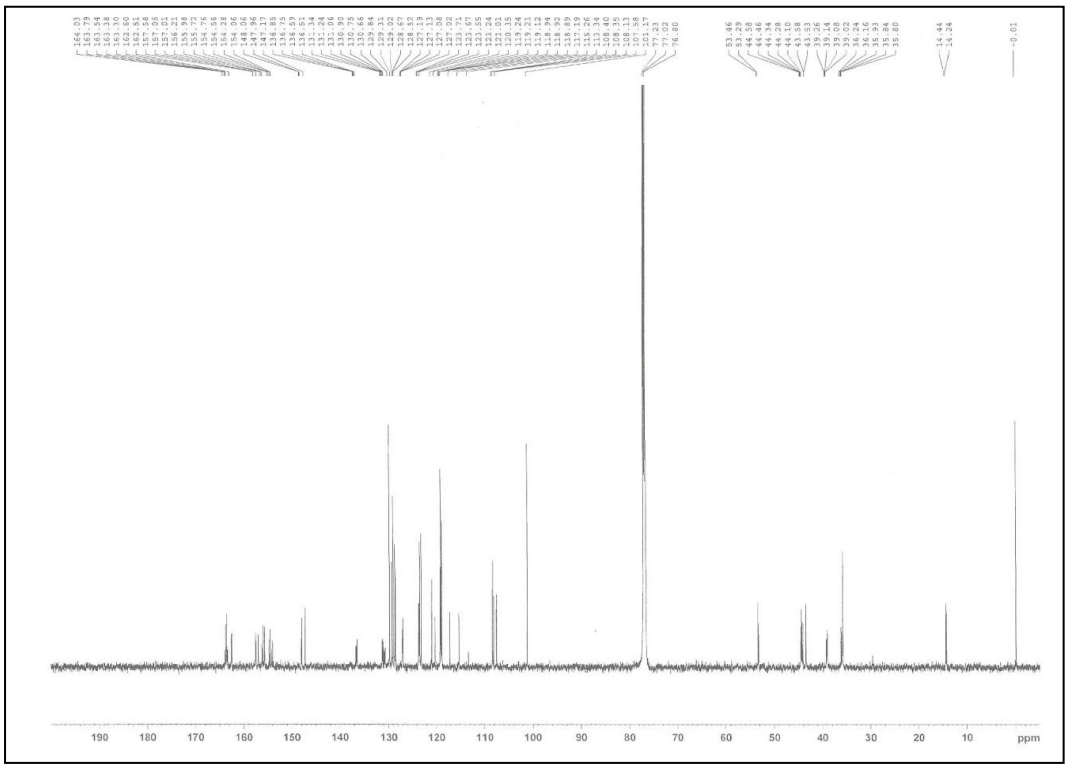

Q2